OPEN ACCESS Freely available online

PLOS | ONE

Anti-Influenza Activity of C_{60} Fullerene Derivatives

Masaki Shoji[1], Etsuhisa Takahashi[2], Dai Hatakeyama[1], Yuma Iwai[1], Yuka Morita[1], Riku Shirayama[1], Noriko Echigo[1], Hiroshi Kido[2], Shigeo Nakamura[3], Tadahiko Mashino[4], Takeshi Okutani[1], Takashi Kuzuhara[1]*

1 Laboratory of Biochemistry, Faculty of Pharmaceutical Sciences, Tokushima Bunri University, Yamashiro-cho, Tokushima, Japan, **2** Division of Enzyme Chemistry, Institute for Enzyme Research, The University of Tokushima, Tokushima, Japan, **3** Department of Chemistry, Nippon Medical School, Nakahara-ku, Kawasaki, Kanagawa, Japan, **4** Department of Pharmaceutical Sciences, Faculty of Pharmacy, Keio University, Minato-ku, Tokyo, Japan

Abstract

The H1N1 influenza A virus, which originated in swine, caused a global pandemic in 2009, and the highly pathogenic H5N1 avian influenza virus has also caused epidemics in Southeast Asia in recent years. Thus, the threat from influenza A remains a serious global health issue, and novel drugs that target these viruses are highly desirable. Influenza A RNA polymerase consists of the PA, PB1, and PB2 subunits, and the N-terminal domain of the PA subunit demonstrates endonuclease activity. Fullerene (C_{60}) is a unique carbon molecule that forms a sphere. To identify potential new anti-influenza compounds, we screened 12 fullerene derivatives using an *in vitro* PA endonuclease inhibition assay. We identified 8 fullerene derivatives that inhibited the endonuclease activity of the PA N-terminal domain or full-length PA protein *in vitro*. We also performed *in silico* docking simulation analysis of the C_{60} fullerene and PA endonuclease, which suggested that fullerenes can bind to the active pocket of PA endonuclease. In a cell culture system, we found that several fullerene derivatives inhibit influenza A viral infection and the expression of influenza A nucleoprotein and nonstructural protein 1. These results indicate that fullerene derivatives are possible candidates for the development of novel anti-influenza drugs.

Citation: Shoji M, Takahashi E, Hatakeyama D, Iwai Y, Morita Y, et al. (2013) Anti-Influenza Activity of C_{60} Fullerene Derivatives. PLoS ONE 8(6): e66337. doi:10.1371/journal.pone.0066337

Editor: Paul Digard, University of Edinburgh, United Kingdom

Received January 10, 2013; **Accepted** May 3, 2013; **Published** June 13, 2013

Funding: This study was supported by the Japan Society for the Promotion of Science (grant no. 20890273, 22590422, 22790098, and 23780051). The funders had no role in study design, data collection and analysis, decision to publish, or preparation of the manuscript.

Competing Interests: The authors have declared that no competing interests exist.

* E-mail: kuzuhara@ph.bunri-u.ac.jp

Introduction

In 1918, an influenza A pandemic caused 50 million deaths worldwide [1], and the development of strategies that can be used to prevent future expansions of this virus continues to be an important endeavor [2]. The avian H5N1 influenza A virus is highly pathogenic to humans [3], and the emergence of a new strain of this virus in 2009, the swine-originating A/H1N1 pdm influenza virus, further emphasizes that this issue is a serious global health problem [4,5]. Although inhibitors of influenza A, e.g., the neuraminidase-like compound oseltamivir, are widely used as antiviral drugs [6,7], the adverse effects of these agents and the emergence of viral strains that are resistant to these drugs have now been reported [8,9].

To prevent and control influenza outbreaks, the development of novel antiviral drugs that are not based on neuraminidase inhibition is now regarded as critical. The influenza A genome consists of segmented single-stranded RNA (-), and its transcription and replication require the activity of a highly conserved RNA-dependent RNA polymerase [10,11]. This polymerase is essential for the propagation of the influenza A virus and is a very promising target for the development of antiviral drugs. The influenza A virus RNA polymerase is composed of three subunits–PA, PB1, and PB2 [12]–and synthesizes viral mRNA using short capped primers that are cleaved from the host's cellular pre-mRNAs by the viral endonuclease [13,14]. Yuan et al. and Dias et al. have shown that the N-terminal domain of the PA subunit contains the active site of the endonuclease, and that this domain also harbors RNA/DNA endonuclease activity [13,14]. Hence, we speculate that PA endonuclease would contain very effective targets for the development of novel anti-influenza A drugs, as we have shown that several chemicals, e.g., catechins, phenethylphenyl phthalimide analogs, and marchantin analogs, inhibit this endonuclease and possess antiviral activity [15–17].

Fullerene (C_{60}), a carbon buckyball, was discovered by Harold Kroto, James R. Heath, Sean O'Brien, Robert Curl, and Richard Smalley in 1985 [18]. It has since been utilized in electronic and mechanical applications [19]. In physiological studies, the biological effects of water-soluble fullerene derivatives containing several hydrophilic groups are noteworthy because fullerene itself is water-insoluble. Water-soluble fullerene derivatives are known to possess various biological and pharmacological properties, including antioxidant activity and inhibitory effects against human immunodeficiency virus (HIV) proteases and DNA photocleavage [20–23]. Mashino et al. also demonstrated that pyrrolidinium fullerene derivative 6 (Fig. 1) has antiproliferative and antibacterial activity [24], malonic acid fullerene derivative 2 (Fig. 1) has excellent antioxidant activity [25], and proline-modified fullerene derivative 3 (Fig. 1) inhibits HIV-reverse transcriptase [22]. Thus, fullerene derivatives are expected to become a novel type of medication because of their unique skeleton.

In our current study, we used an *in vitro* influenza PA endonuclease assay to analyze the effects of 12 different fullerene derivatives on the endonuclease activity of the PA N-terminal

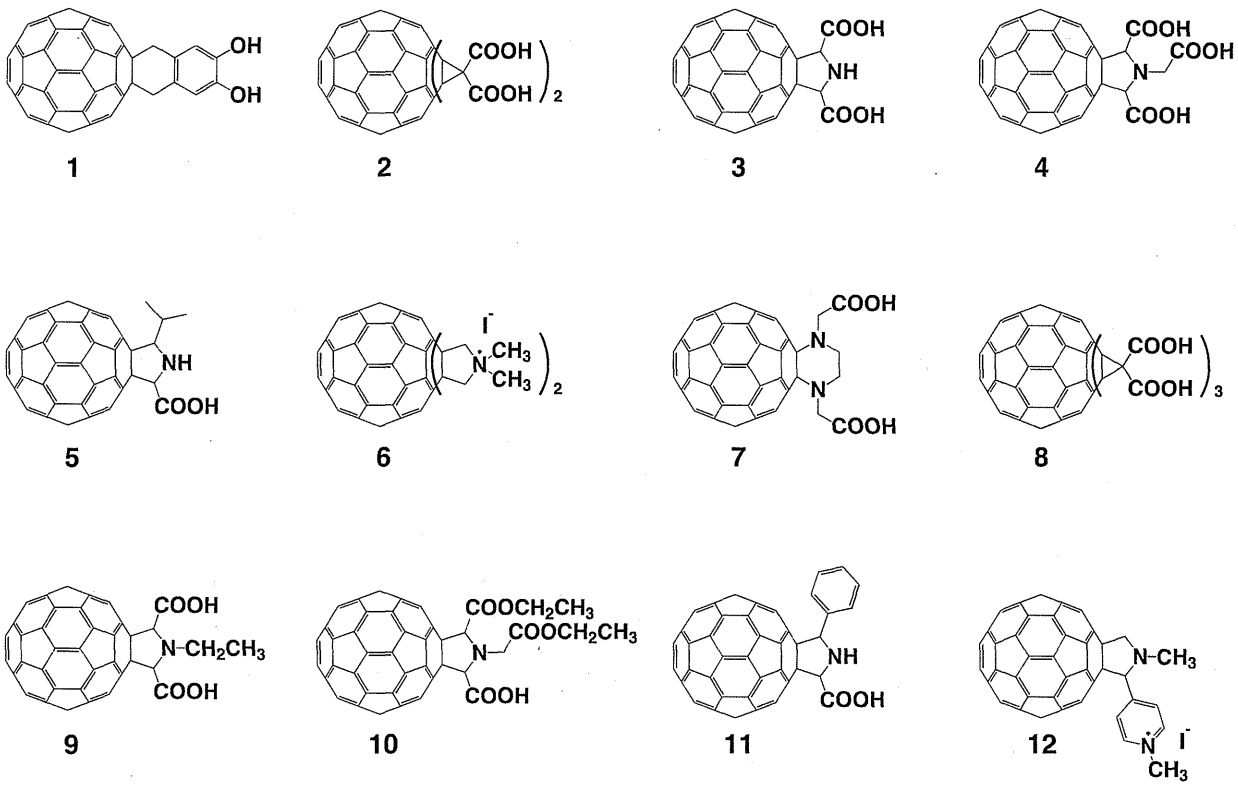

Figure 1. Chemical structures of the C60 fullerene derivatives tested in this study. The chemical structures of the fullerene derivatives examined in this study are shown. The sources for these structures are described in the Materials and Methods. No. 1, 1,4-dihydro-6,7-dihydroxy [60]fullerenonaphthlene; no. 2, [60]fullerenodicyclopropane-1,1,1′,1′-tetracarboxylic acid; no. 3: [60]fullerenopyrrolidine-2,5-dicarboxylic acid; no. 4, 1-carboxymethyl [60]fullerenopyrrolidine-2,5-dicarboxylic acid; no. 5, 5-isopropyl [60]fullerenopyrrolidine-2-carboxylic acid; no. 6:1,1,1′,1′-tetramethyl [60]fullerenodipyrrolidinium diiodide; no. 7, [60]fullerenopiperazine-1,4-diacetic acid; no. 8: [60]fullerenotricyclopropane-1,1,1′,1′,1′′,1′′-hexacarboxylic acid; no. 9, 1-ethyl [60]fullerenopyrrolidine-2,5-dicarboxylic acid; no. 10, 1-ethoxycarbonylmethyl [60]fullerenopyrrolidine-2,5-dicarboxylic acid 2-ethyl ester; no. 11, 5-phenyl [60]fullerenopyrrolidine-2-carboxylic acid; and no. 12, 4-(1′-methyl [60]fullerenopyrrolidin-2′-yl)-1-methylpyridinium iodide.

doi:10.1371/journal.pone.0066337.g001

domain and full-length PA. We found that the fullerene derivatives inhibit influenza PA endonuclease activity and viral infection. Our results indicate the possibility of developing fullerene derivatives into novel anti-influenza A drugs in the future.

Results

Inhibition of PA Endonuclease by Fullerene Derivatives

For the *in vitro* PA endonuclease assay, we expressed and purified a recombinant influenza PA endonuclease domain (1–220 residues; Fig. 2A, B) using bacteria as described previously [15–17]. For the assay, we incubated 0.1 μM recombinant PA endonuclease domain with 1 or 10 μM of each fullerene derivative (Fig. 2C). The PA endonuclease domain digested M13 mp18 circular single-stranded DNA *in vitro* (Fig. 2C, lanes 1 and 2) [12–16], and we investigated whether any of the fullerene derivatives could inhibit this activity. The fullerene derivatives 2–5, 7, 8, 10, and 11 significantly inhibited the digestion of M13 mp18 at a dose of 10 μM, no. 12 slightly inhibited digestion, and no. 1, 6, and 9 had no or weak inhibitory activity (Fig. 2C). This is the first study to report that fullerene derivatives can inhibit the activity of influenza enzymes. Fullerene derivative no. 6 caused a mobility shift of M13 mp18, possibly because it has a cationic amine group (Fig. 2C, lane 13). The solubility of the fullerene derivatives 1 and 6 in water was relatively low, which might have been the cause of their decreased activity levels.

To investigate the effects of full-length PA protein on PA endonuclease activity and the inhibitory activity of the fullerene derivatives, we examined whether the fullerene derivatives also inhibit the endonuclease activity of full-length PA protein. We expressed the recombinant full-length PA protein by using a baculovirus to infect Sf9 insect cells (Fig. 3A) and purified it using a Ni-agarose and HiTrap-Q column (Fig. 3B). The recombinant full-length PA protein demonstrated endonuclease activity (Fig. 3C, lanes 1 and 2) [26,27]. Then, we tested the 12 fullerene derivatives using this same assay. The fullerene derivatives 2–5, 7, 8, 10, and 11 inhibited the endonuclease activity of full-length PA (Fig. 3C), which is consistent with the results for the PA endonuclease domain (Fig. 2C). The M13 mp18 band in the no. 12-treated lane was degraded (Fig. 3C lane 14), the band in the no. 1 and 9-treated lanes slightly remained (Fig. 3C, lanes 3 and 11), suggesting that fullerene derivatives no. 1 and 9 also slightly inhibited the PA endonuclease activity of the full length PA protein.

As shown in Figs. 2C and 3C, the M13 mp18 band in the no. 6-treated lanes shifted and was clear (Fig. 3C lane 8), respectively, suggesting that no. 6 has the ability to cleave DNA. Thus, we examined the nuclease activity of the fullerene derivatives (Fig. 4). The result showed that fullerene derivative no. 6 by itself has

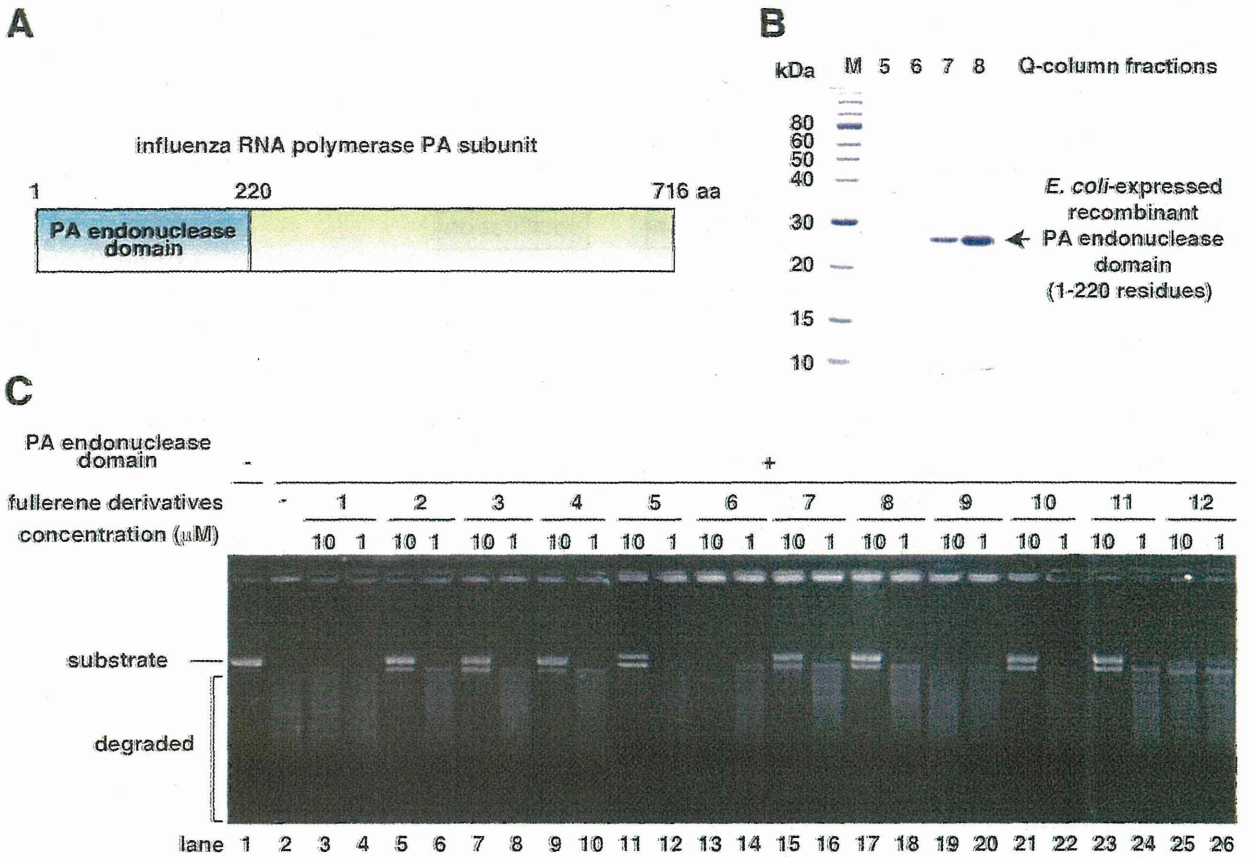

Figure 2. Inhibition of the activity of the PA endonuclease domain by the fullerene derivatives. (**A**) Schematic of the PA subunit of influenza RNA polymerase. (**B**) Purification of the bacterially expressed PA endonuclease domain using a HiTrap-Q column. The arrow indicates the PA endonuclease domain. (**C**) The effects of the various fullerene derivatives on the endonuclease activity of the PA N-terminal domain of the influenza A RNA polymerase were tested. The recombinant PA N-terminal domain protein was added to each reaction at a concentration of 0.25 μg/100 μL. A zero control (i.e., no PA domain added) was also assayed. The fullerene derivatives were added at a dose of 1 or 10 μM, and M13 mp18 was used as the substrate.
doi:10.1371/journal.pone.0066337.g002

significant nuclease activity in the absence of PA endonuclease (Fig. 4). No. 12 also showed weaker nuclease activity by itself (Fig. 4).

Docking Simulation of Influenza A Endonuclease and C_{60} Fullerene

Previously, we reported that 3 of 34 phthalimide chemicals and 5 of 33 phytochemicals inhibited PA endonuclease activity [12,15,16]. In the case of the fullerenes, 8 of the 12 fullerene derivatives inhibited PA endonuclease activity; thus, we thought that the fullerene skeleton itself could fit into the active pocket of the influenza PA endonuclease domain. To investigate how the fullerene molecule binds to and fits in the active pocket of the PA endonuclease domain, we performed *in silico* docking simulation analysis of this interaction at the level of the tertiary structure using Molecular Operating Environment software (MOE; Chemical Computing Group, Quebec, Canada) [28]. The results show that fullerene fits into and fills the active pocket of the endonuclease domain of the influenza RNA polymerase (Fig. 5A), suggesting that this may be the major cause of the inhibitory mechanism. The two divalent ions of manganese in the active pocket are reportedly necessary for influenza endonuclease activity [13,14]. Fullerene binds to manganese ions by arene-cation interactions at the back of the active pocket (Fig. 5B and 5C), suggesting that this binding is also one of the inhibitory mechanisms.

Toxicity of the Fullerene Derivatives Against the Madin-Darby Canine Kidney Cell Line

We evaluated the toxicity of the fullerene derivatives against Madin-Darby canine kidney (MDCK) cells before examining their antiviral activity against the influenza A virus. Various concentrations (12.5–100 μM) of the fullerene derivatives were added to cultures of MDCK cells. Marchantin E (ME) was used as the positive controls for anti-influenza activity [16]. At 24 h post-incubation, the cell viability of the treated-cells was determined using an MTT cell proliferation assay (Fig. 6A). The viability of the cells treated with the fullerene derivatives 1–12 and ME was not significantly different to that of the cells treated with dimethyl sulfoxide (DMSO) at a concentration of 12.5 to 100 μM. We also performed naphthol blue black assay for cytotoxicity of fullerene derivatives (Fig. 6B). At 24 h post-incubation, the viable cells were stained using a blue dye. The wells treated with 0.8–100 μM of the fullerene derivatives 1–12 and DMSO were stained blue (Fig. 6B). Taken together, these data show that the fullerene derivatives (1–12) are not toxic to MDCK cells up to a concentration of 100 μM.

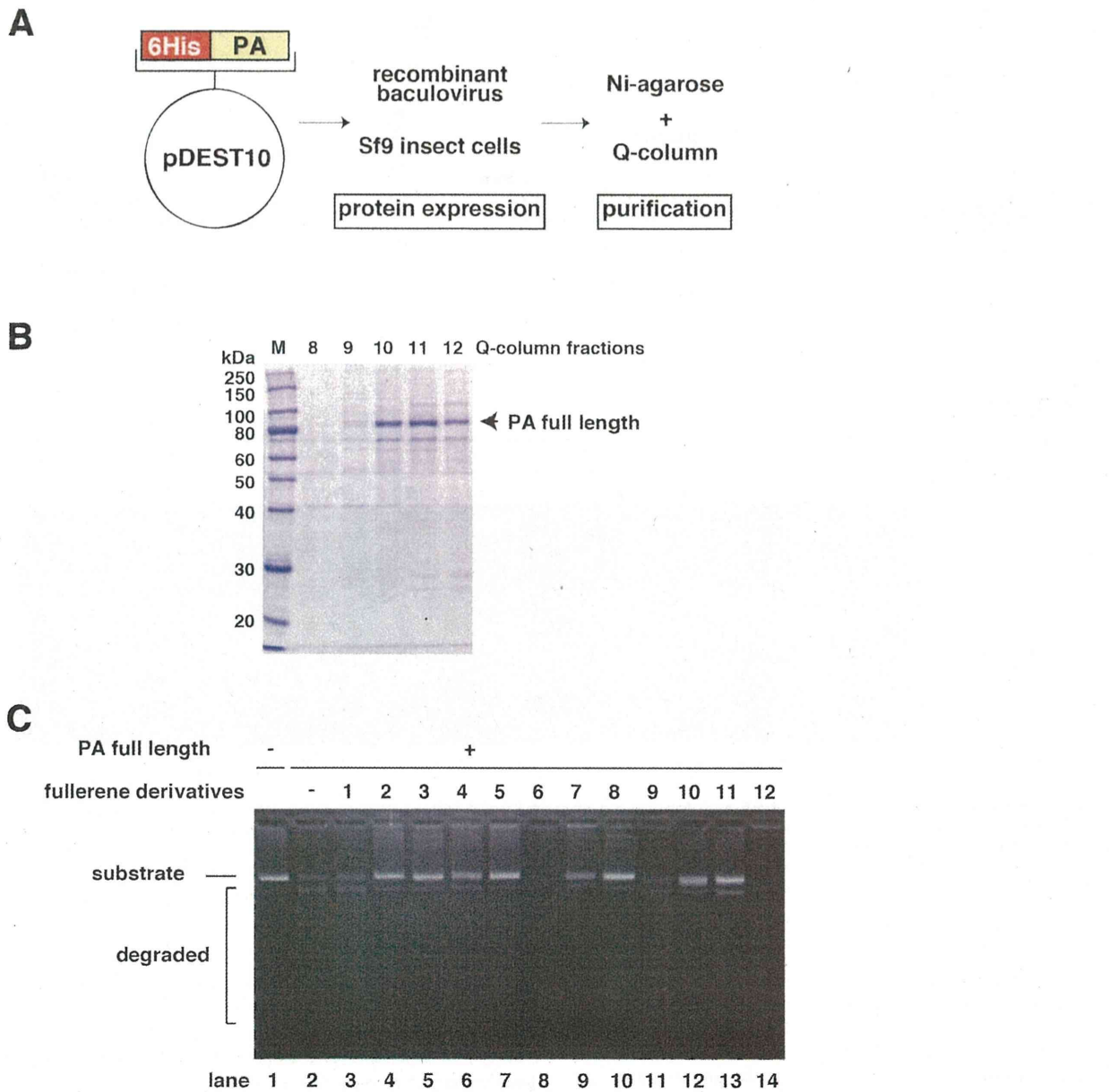

Figure 3. Inhibition of the activity of full-length PA endonuclease by the fullerene derivatives. (**A**) Schematic of the constructed plasmid, baculovirus expression, and purification of full-length PA protein. (**B**) Purification of full-length PA protein using a HiTrap-Q column. The numbers indicate the fractions. The arrow indicates full-length PA protein. (**C**) The effects of the various fullerene derivatives on the endonuclease activity of full-length PA protein of influenza A RNA polymerase were tested. Recombinant full-length PA protein was added to each reaction at a concentration of 0.25 μg/100 μL. A zero control (i.e., no PA protein added) was also assayed. The fullerene derivatives were added at a dose of 10 μM and M13 mp18 was used as the substrate.
doi:10.1371/journal.pone.0066337.g003

Inhibition of Influenza A Virus Infection by the Fullerene Derivatives

We evaluated the antiviral activity of the fullerene derivatives against the influenza A virus (A/Puerto Rico (PR)/8/34 (H1N1) or A/Aichi/2/68 (H3N2)). Various concentrations of the fullerene derivatives and the virus were mixed and added to cultures of MDCK cells [29]. ME and DMSO were used as positive and negative controls for the inhibitory effect of influenza A virus infection, respectively. At 24 h post-infection, we performed influenza A nucleoprotein (NP)-immunostaining of the treated cells, and the stained cells were counted. At 100 μM, fullerene derivatives no. 2–8, 11 and 12 significantly reduced the number of NP-positive cells in comparison with the control (DMSO), in A/PR8/34 (H1N1)-infected cells (Fig. 7A & C). Also in A/Aichi/2/68 (H3N2)-infected cells, at 100 μM, fullerene derivatives no. 2–8 and 10–12 significantly reduced the number of NP-positive cells in comparison with the DMSO (Fig. 7B & D). The fullerene derivatives 10 in A/PR8/34 (H1N1) also slightly decreased the

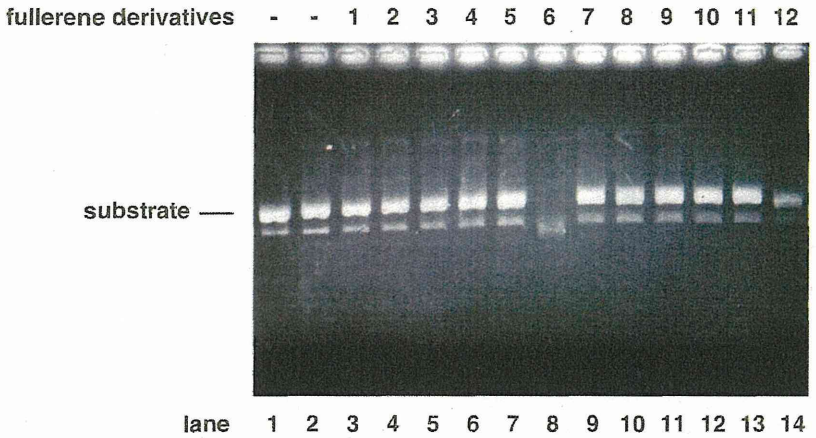

Figure 4. Nuclease activity of the fullerene derivatives. The method was the essentially same as that of Figs. 2 & 3, except the condition of the absence of PA protein. The fullerene derivatives were added at a dose of 10 μM and M13 mp18 was used as the substrate. The digestion of the substrate was examined by agarose electrophoresis.
doi:10.1371/journal.pone.0066337.g004

number of NP-positive cells (Fig. 7A & C). Conversely, the number of NP-positive cells treated with the fullerene derivatives 1 and 9 were comparable to that of the DMSO-treated cells (Fig. 7A–D).

Based on these results, to compare their activities quantitatively, we calculated IC_{50} values of fullerene derivatives against A/PR8/34 (H1N1) and A/Aichi/2/68 (H3N2) strains. Against H1N1 PR8 strain, IC_{50} values are as follows: 57 μM for fullerene derivatives no. 2; 70 μM for no. 4; 37 μM for no. 5; 20 μM for no. 6; 37 μM for no. 8; 44 μM for no. 11; 78 μM for no. 12; more than 100 μM for no. 3, 7 or 10; 43 μM for ME (Table 1). Against H3N2 Aichi strain, IC_{50} values: 91 μM for fullerene derivatives no. 4; 31 μM for no. 6; 63 μM for no. 12; more than 100 μM for no. 2, 3, 5, 7, 8, 10 or 11; 53 μM for ME (Table 1). IC_{50} values of fullerene derivatives no. 1 or 9 could not be calculated against the strains because of their weak activities (Table 1). Taken together, it indicated that several fullerene derivatives have stronger anti-influenza activity than ME.

Moreover, we examined the expression levels of viral proteins by western blotting of treated-cell lysates in A/PR8/34 (H1N1)-infected wells at 4, 8, 12 (Fig. 8A), and 24 h (Fig. 8B) post-infection. The expression levels of influenza A NP and nonstructural protein 1 (NS1) proteins in the cells treated with the fullerene derivatives 5, 6, and 11, and ME were reduced as compared with that of the DMSO-treated cells, but slightly reduced in the wells

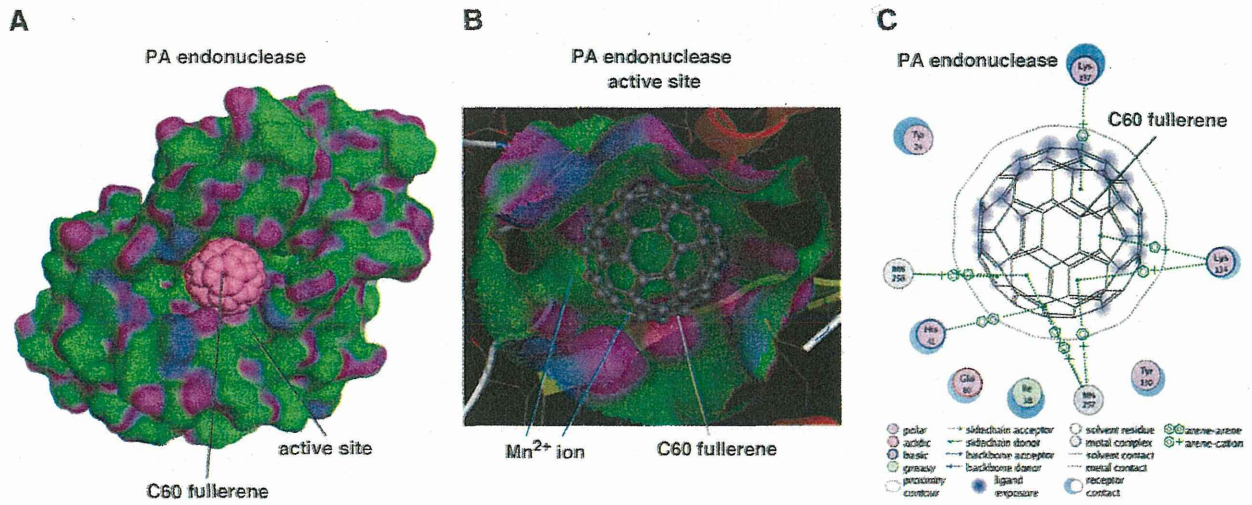

Figure 5. Docking simulation of C_{60} fullerene with influenza PA endonuclease. (**A**) Docking simulation analysis of C_{60} fullerene with the PA endonuclease domain of influenza A RNA polymerase. The fullerene is shown as a sphere. The surface of the pocket of PA endonuclease is shown in green and purple. The pink ball indicates the carbon atoms in the fullerene. (**B**) The fitting of the fullerene to the active pocket of PA endonuclease. PA endonuclease is depicted as a ribbon structure. The α-helix and β-strands are shown in red and yellow, respectively. The fullerene is shown as a gray stick structure. The manganese ions in PA endonuclease are behind the fullerene. (**C**) Two-dimensional analysis of the interactions between fullerene and PA endonuclease. The fullerene is shown in the center with the key and with the interacting amino acids shown around it. MN indicates the Mn^{2+} ions. The modes of interaction are shown at the bottom. The arene of the fullerene interacts with 2 Mn^{2+} ions and the amino acids, e.g., lysine and histidine, in PA endonuclease.
doi:10.1371/journal.pone.0066337.g005

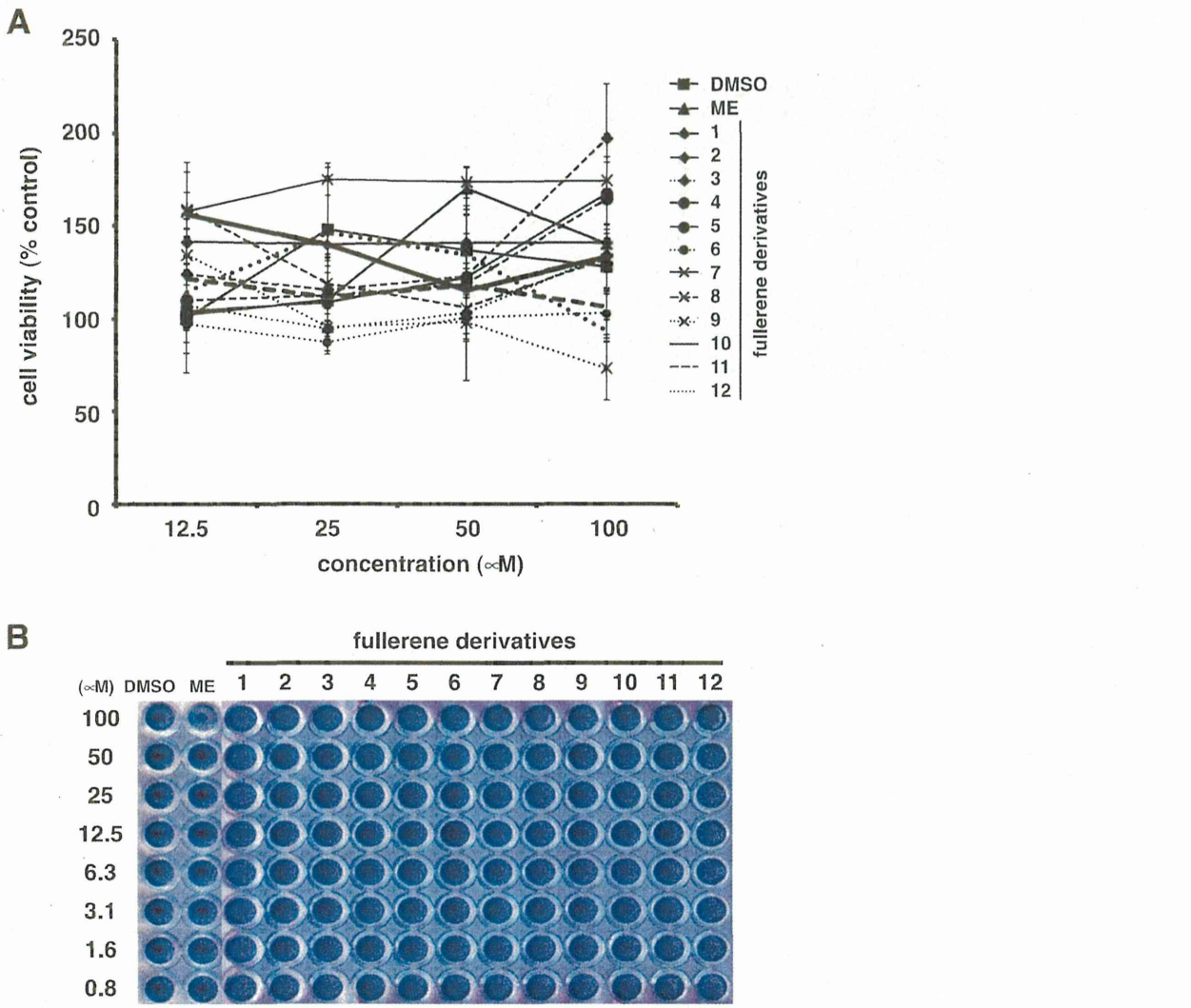

Figure 6. Toxicity of the fullerene derivatives against MDCK cells. (**A**) Various concentrations (12.5–100 μM) of the fullerene derivatives (n = 4) were added to cultures of MDCK cells. DMSO and ME were used as negative and positive controls for anti-influenza activity, respectively. At 24 h post-incubation, cell viability was determined using an MTT cell proliferation assay. Data represent the mean ± standard error of the mean (S.E.M.). (**B**) Various concentrations (0.8–100 μM) of the fullerene derivatives were added to cultures of MDCK cells. ME was used as positive control for cytotoxicity. At 24 h post-incubation, the cells were fixed and viable cells were stained with a naphthol blue black solution.
doi:10.1371/journal.pone.0066337.g006

treated with the fullerene derivatives 2–5, 7, 8, 10 and 12 (Fig. 8A and 8B). Conversely, the expression levels of influenza A NP and NS1 proteins in cells treated with the fullerene derivatives 1 and 9 were comparable to those in the DMSO-treated cells (Fig. 8A and 8B). Taken together, these data show that the fullerene derivatives 2–8 and 10–12 possess antiviral effects against the influenza A virus, and their mechanism of action may be by the inhibition of PA endonuclease activity (no. 2–5, 7, 8, and 11) or their ability to cleave viral RNA (no. 6 and 12).

Discussion

In this study, we showed that the fullerene derivatives 2–5, 7, 8, 10, and 11 or 6 and 12 possess inhibitory activity against influenza PA endonuclease or the ability to cleave DNA, respectively. Moreover, we showed that the fullerene derivatives 2–8 and 10–12 inhibit the infection of the influenza A virus. Above all, no. 6 showed the strongest antiviral activity. A previous report showed that certain fullerene derivatives have DNA and RNA cleavage activity [20,30]. As shown in Figs. 2C and 3C, the M13 mp18 band in the no. 6-treated lanes shifted and was clear, respectively. Since no. 6 has the activity to cleave DNA, the antiviral activity of no. 6 may be caused by its cleavage of viral RNA. Therefore, fullerene derivatives are promising novel anti-influenza chemicals. These data are an important advance that could be used in future strategies to refine fullerene-based drug designs. Our analysis provides valuable new information for the design of novel anti-influenza drugs. There was no correlation between the PA endonuclease and antiviral activity of fullerene derivative no. 12. This may be because it targets influenza A virus attachment/entry or growth in cells and also because of differences in its permeability into the cells. When we performed the anti-viral experiment without pre-incubation, we could not find an

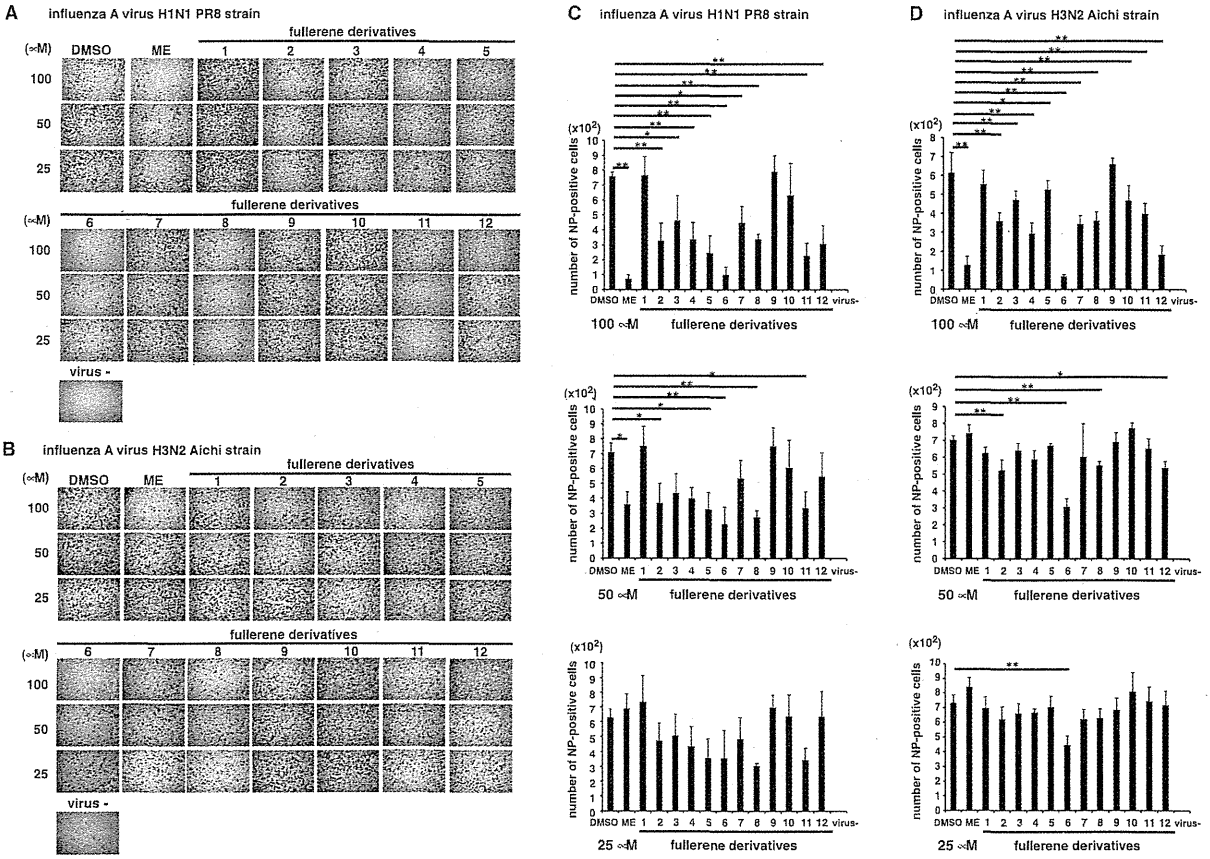

Figure 7. Immunostaining of influenza A virus-infected cells. Various concentrations of the fullerene derivatives (25–100 μM) and an MOI of 1 influenza A virus (A/PR/8/34 (H1N1) (n = 3) (**A and C**) or A/Aichi (H3N2) (n = 4) (**B and D**)) were mixed and added to cultures of MDCK cells. At 24 h post-infection, influenza A NP-immunostaining of the treated cells was performed. The wells were photographed under a microscope (×4) (**A and B**), and the stained cells were counted (**C and D**). DMSO (n = 4) and ME (n = 4) were used as negative and positive controls for the inhibitory effect of influenza A virus infection, respectively. Data represent the mean ± S.E.M. $*p<0.05$, $**p<0.01$.
doi:10.1371/journal.pone.0066337.g007

experimental condition under which the fullerene derivatives showed anti-virus activity. This suggests that the fullerene derivatives may have virucidal activity or they may enter cells by associating with the virus.

Other groups also have reported novel anti-influenza polymerase inhibitors such as T-705 and L-742,001 [27,31–36], which are substituted pyrazine and piperidine compounds, respectively. Since the chemical structures of fullerene derivatives are completely different from those of them, indicating that fullerene derivatives are quite novel anti-influenza compounds.

Finally, we conclude that the chemical and biochemical information presented here will be very useful for the future development of novel fullerene-based drugs against influenza A.

Materials and Methods

Preparation of the C_{60} Fullerene Derivatives

Water-soluble fullerene derivatives were synthesized and purified using previously reported methods with small modifications [20–25]. All of the fullerene derivatives were dissolved in DMSO to a concentration of 10 mM as stock solutions. The fullerene derivatives (Fig. 1) used in these experiments consisted of the following [20–25]: no. 1, 1,4-dihydro-6,7-dihydroxy [60]fullerenonaphthlene; no. 2, [60]fullerenodicyclopropane-1,1,1′,1′-tetracarboxylic acid; no. 3, [60]fullerenopyrrolidine-2,5-dicarboxylic acid; no. 4, 1-carboxymethyl [60]fullerenopyrrolidine-2,5-dicarboxylic acid; no. 5, 5-isopropyl [60]fullerenopyrrolidine-2-carboxylic acid; no. 6, 1,1,1′,1′-tetramethyl [60]fullerenodipyrrolidinium diiodide; no. 7, [60]fullerenopiperazine-1,4-diacetic acid; no. 8, [60]fullerenotricyclopropane-1,1,1′,1′,1′′,1′′′-hexacarboxylic acid; no. 9, 1-ethyl [60]fullerenopyrrolidine-2,5-dicarboxylic acid; no. 10, 1-ethoxycarbonylmethyl [60]fullerenopyrrolidine-2,5-dicarboxylic acid 2-ethyl ester; no. 11, 5-phenyl [60]fullerenopyrrolidine-2-carboxylic acid; and no. 12, 4-(1′-methyl [60]fullerenopyrrolidin-2′-yl)-1-methylpyridinium iodide.

Bacterial Expression and Purification of the PA Endonuclease Domain

The influenza A virus (A/PR/8/34 (H1N1)) RNA polymerase PA plasmid, pBMSA-PA, was obtained from the DNA bank at Riken BioResource Center (Tsukuba, Japan; originally deposited by Susumu Nakada) [37]. The cDNA fragment corresponding to the PA N-terminal endonuclease domain (residues 1–220; Fig. 2A) was amplified by polymerase chain reaction (PCR) [38] from pBMSA-PA. The amplified product was subcloned into the pET28a (+) plasmid (Novagen, Madison, WI, USA). The induction of recombinant protein expression was achieved by the addition of isopropyl-D-thiogalactopyranoside [39], and this

Table 1. IC_{50} of the fullerene derivatives against influenza A virus H1N1 and H3N2 strains.

		IC_{50} (μM)	
		H1N1 PR8 strain	H3N2 Aichi strain
Marchantin E		43	53
Fullerene derivatives	no. 1	ND	ND
	no. 2	57	>100
	no. 3	>100	>100
	no. 4	70	91
	no. 5	37	>100
	no. 6	20	31
	no. 7	>100	>100
	no. 8	37	>100
	no. 9	ND	ND
	no. 10	>100	>100
	no. 11	44	>100
	no. 12	78	63

ND: not detected.
doi:10.1371/journal.pone.0066337.t001

was followed by purification using Ni^{2+}-agarose [40]. The recombinant PA endonuclease domain protein was further purified to near homogeneity (Fig. 2B) using a HiTrapQ-FF column (GE Healthcare, Buckinghamshire, UK).

Baculoviral Expression and Purification of the Full-length PA Subunit

The cDNA fragment corresponding to the full-length protein-coding region of PA was amplified by PCR [38] from pBMSA-PA using the primers PA_start_TOPO (CAC CAT GGA AGA TTT TGT GCG AC), PA stop (CTA ACT CAA TGC ATG TGT AAG), PA_mid_anti (TCT TTG GAC ATT TGA GAC AG), and PA_mid_TOPO (CAC CAA TTG AAG AAA GGT TTG). The amplified product was then subcloned into the pENTR/D-TOPO plasmid (Gateway®, Life Technologies™, Carlsbad, CA, USA) using topoisomerase I cloning. The resulting construct was then converted to pDEST10-PA using the clonase (Fig. 3A). The plasmid was transfected into Sf9 insect cells using the helper virus. The resultant baculovirus was again transfected into Sf9 cells [41]. The expressed full-length PA protein was purified using Ni^{2+}-agarose and a HiTrap Q FF column (GE Healthcare) with the AKTA prime plus system (Fig. 3B).

PA Endonuclease Activity and Fullerene Derivatives Nuclease Assays

Influenza A RNA polymerase PA endonuclease activity assays were performed as described by Dias et al. with some modifications [12–16]. Briefly, the pH was lowered from 8.0 to 7.3, and 1 μg M13 mp18 single-stranded circular phage DNA was used as the substrate. A total of 0.25 μg recombinant PA endonuclease domain or full-length PA protein were added to 100 μL assay buffer for each reaction (the final concentration of the protein was approximately 0.1 μM). For the fullerene derivative nuclease assay, no PA protein was added at this step. The fullerene derivatives (summarized in Fig. 1) were then added to the reaction, and the products were analyzed by agarose electrophoresis and stained with ethidium bromide.

In Silico Docking Simulation Analysis of Fullerene C_{60} and the PA Endonuclease Domain of Influenza RNA Polymerase

All molecular modeling studies were performed using MOE software (Chemical Computing Group) [26,42,43]. Information regarding the tertiary structure of the influenza PA endonuclease domain (PDB ID: 3HW6) was obtained from a protein data bank [29]. This enzyme was prepared for docking studies in which (1)

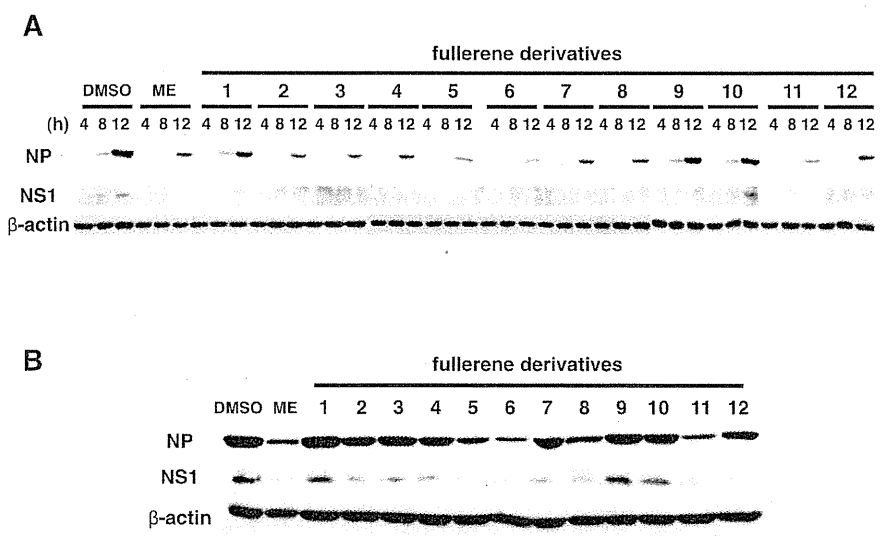

Figure 8. Expression levels of influenza A viral proteins. We mixed 100 μM of the fullerene derivatives or ME and an MOI of 1 influenza A virus (A/PR/8/34 (H1N1)) and added the mixture to cultures of MDCK cells. At 4, 8, 12 (**A**), and 24 h (**B**) postinfection, the expression levels of influenza A NP and NS1 proteins in treated-cell lysates were analyzed by western blotting, and β-actin was analyzed as an internal control. The experiments were performed three times and the results were reproducible.
doi:10.1371/journal.pone.0066337.g008

the ligand molecule was removed from the active site of the enzyme; (2) hydrogen atoms were added to the structure using standard geometry; (3) the structure was minimized using an MMFF94s force-field; (4) MOE Alpha Site Finder was used to search for active sites within the enzyme structure and dummy atoms were created from the obtained alpha spheres; and (5) the obtained model was then used in the Dock program (Ryoka Systems Inc., Tokyo, Japan). The conformation of the fullerene was generated by systematic, stochastic searches and Low Mode MD (molecular dynamics).

MTT Cell Proliferation Assay

The cytotoxicity of the fullerene derivatives in MDCK cells was determined with an MTT cell proliferation assay kit according to the manufacturer's instructions (Cayman, Arbor, MI, USA). Briefly, MDCK cells were cultured in Dulbecco's modified Eagle medium (DMEM; Gibco/Invitrogen, Carlsbad, CA, USA) supplemented with 10% fetal bovine serum, 1% penicillin-streptomycin, and 4 mM L-glutamine at 37°C under 5% CO_2. A confluent monolayer of MDCK cells was prepared in each well of a 96-well plate. Various concentrations (12.5–100 μM) of the fullerene derivatives and ME in DMSO (100 μM chemicals: 1%, 50 μM: 0.5%, 25 μM: 0.25%, 12.5 μM: 0.125%.), which were used as the anti-influenza activity [16], were mixed in an infection medium (DMEM supplemented with 1% bovine serum albumin, 1% penicillin-streptomycin, and 4 mM L-glutamine). The mixture was added to the cells, and the treated cells were incubated for 24 h at 37°C under 5% CO_2. After incubation, the cells were treated with the MTT reagent and incubated for 4 h at 37°C under 5% CO_2. The wells were treated with the crystal dissolving solution to lyse the formazan produced in the cells, and the absorbance of each well was measured at 570 nm using a microplate reader.

Cytotoxicity Assay by Naphthol Blue Black

A confluent monolayer of MDCK cells was prepared in each well of a 96-well plate. Various concentrations (0.8–100 μM) of the fullerene derivatives in DMSO were mixed with an infection medium (DMEM supplemented with 1% bovine serum albumin, 1% penicillin-streptomycin, and 4 mM L-glutamine) and incubated for 30 min at 37°C under 5% CO_2 [43]. The mixture was added to the cells, and the treated cells were incubated for 24 h at 37°C under 5% CO_2. After incubation, the cells were fixed using a 10% formaldehyde solution. Viable cells were stained with a naphthol blue black solution (0.1% naphthol blue black, 0.1% sodium acetate, and 9% acetic acid) [43].

Immunostaining of Influenza A Virus-infected Cells

MDCK cells were prepared in each well of a 96-well plate. Various concentrations (25–100 μM) of the fullerene derivatives and ME were mixed at a multiplicity of infection (MOI) of 1 influenza A virus (A/PR/8/34 (H1N1) or A/Aichi/2/68 (H3N2)) in the infection medium and incubated for 30 min at 37°C under 5% CO_2. The mixture was added to the cells, and the treated cells were incubated for 24 h at 37°C under 5% CO_2. After incubation, the cells were fixed with 4% paraformaldehyde in phosphate-buffered saline (-) for 30 min at 4°C and then permeabilized with 0.3% Triton X-100 for 20 min at room temperature. A mouse anti-influenza A NP antibody (FluA-NP 4F1; SouthernBiotech, Birmingham, AL, USA) and horseradish peroxidase-conjugated goat anti-mouse IgG antibody (SouthernBiotech) were used as primary and secondary antibodies, respectively [44]. To visualize the infected cells, TrueBlue peroxidase substrate (KPL, Gaithersburg, MD, USA) was added, and color development was terminated after 15 min of incubation by washing with H_2O. The wells were photographed under a microscope, and the stained cells were counted.

Western Blotting

MDCK cells were prepared in each well of a 24-well plate. We mixed 100 μM of the fullerene derivatives and ME at an MOI of 1 influenza A virus (A/PR/8/34 (H1N1)) in the infection medium and incubated the solution for 30 min at 37°C under 5% CO_2. The mixture was added to the cells, and the treated cells were incubated for 4, 8, 12, and 24 h at 37°C under 5% CO_2. After incubation, the cells were lysed with a sodium dodecyl sulfate buffer (125 mM Tris-HCl, pH 6.8, 5% sodium dodecyl sulfate, 25% glycerol, 0.1% bromophenol blue, and 10% β-mercaptoethanol) and boiled for 5 min. The cell lysates were then loaded onto a 10% polyacrylamide gel. The proteins were transferred to a polyvinylidene fluoride microporous membrane (Millipore, Billerica, MA, USA). For primary antibodies, mouse anti-influenza A NP antibody (FluA-NP 4F1; SouthernBiotech) and goat anti-influenza A NS1 antibody (vC-20; Santa Cruz Biotechnology, Santa Cruz, CA, USA) were used to detect NP and NS1, respectively. A rabbit anti-β–actin antibody (13E5; Cell Signaling, Danvers, MA, USA) was used as an internal control. Horseradish peroxidase-conjugated goat anti-mouse IgG antibody (SouthernBiotech), donkey anti-goat IgG antibody (sc-2020; Santa Cruz Biotechnology) and goat anti-rabbit IgG antibody (KPL) were used as secondary Abs. The blots were developed by using Western Lightning ECL Pro (PerkinElmer, Waltham, MA, USA).

Statistical Analysis

All results were expressed as the mean ± standard error of the mean. Differences were analyzed for statistical significance by one-way analysis of variance (ANOVA) for comparison among the DMSO, ME and fullerene derivative-treated groups. The results were considered significantly different at $*p<0.05$ and $**p<0.01$ when comparing the number of stained cells in the ME or fullerene derivatives-treated groups to that of the DMSO-treated group.

Acknowledgments

The influenza A virus (A/PR/8/34 (H1N1)) RNA polymerase PA plasmid, pBMSA-PA, was provided by the DNA bank at the Riken BioResource Center (Tsukuba, Japan; originally deposited by Susumu Nakada) with the support of the National Bio-Resources Project of the Ministry of Education, Culture, Sports, Science, and Technology of Japan.

Author Contributions

Conceived and designed the experiments: TK. Performed the experiments: MS ET DH YI YM RS NE TO. Analyzed the data: MS ET YI YM RS HK. Contributed reagents/materials/analysis tools: SN TM ET HK. Wrote the paper: TK MS.

References

1. Taubenberger JK, Reid AH, Lourens RM, Wang R, Jin G, et al. (2005) Characterization of the 1918 influenza virus polymerase genes. Nature 437: 889–893.
2. Horimoto T, Kawaoka Y (2005) Influenza: lessons from past pandemics, warnings from current incidents. Nat Rev Microbiol 3: 591–600.
3. Hatta M, Gao P, Halfmann P, Kawaoka Y (2001) Molecular basis for high virulence of Hong Kong H5N1 influenza A viruses. Science 293: 1840–1842.

4. Itoh Y, Shinya K, Kiso M, Watanabe T, Sakoda Y, et al. (2009) *In vitro* and *in vivo* characterization of new swine-origin H1N1 influenza viruses. Nature 460: 1021–1025.
5. Neumann G, Noda T, Kawaoka Y (2009) Emergence and pandemic potential of swine-origin H1N1 influenza virus. Nature 459: 931–939.
6. De Clercq E (2006) Antiviral agents active against influenza A viruses. Nat Rev Drug Discov 5: 1015–1025.
7. Hayden FG, Atmar RL, Schilling M, Johnson C, Poretz D, et al. (1999) Use of the selective oral neuraminidase inhibitor oseltamivir to prevent influenza. N Engl J Med 341: 1336–1343.
8. Collins PJ, Haire LF, Lin YP, Liu J, Russell RJ, et al. (2008) Crystal structures of oseltamivir-resistant influenza virus neuraminidase mutants. Nature 453: 1258–1261.
9. Reece PA (2007) Neuraminidase inhibitor resistance in influenza viruses. J Med Virol 79: 1577–1586.
10. Honda A, Ishihama A (1997) The molecular anatomy of influenza virus RNA polymerase. Biol Chem 378: 483–488.
11. Honda A, Mizumoto K, Ishihama A (2002) Minimum molecular architectures for transcription and replication of the influenza virus. Proc Natl Acad Sci U S A 99: 13166–13171.
12. Kuzuhara T, Iwai Y, Takahashi H, Hatakeyama D, Echigo N (2009) Green tea catechins inhibit the endonuclease activity of influenza A virus RNA polymerase. PLoS Curr Oct. 13: 1:RRN1052.
13. Dias A, Bouvier D, Crépin T, McCarthy AA, Hart DJ, et al. (2009) The cap-snatching endonuclease of influenza virus polymerase resides in the PA subunit. Nature 458: 914–918.
14. Yuan P, Bartlam M, Lou Z, Chen S, Zhou J, et al. (2009) Crystal structure of an avian influenza polymerase PA(N) reveals an endonuclease active site. Nature 458: 909–913.
15. Iwai Y, Takahashi H, Hatakeyama D, Motoshima K, Ishikawa M, et al. (2010) Anti-influenza activity of phenethylphenylphthalimide analogs derived from thalidomide. Bioorg Med Chem 18: 5379–5390.
16. Iwai Y, Murakami K, Gomi Y, Hashimoto T, Asakawa Y, et al. (2011) Anti-influenza activity of marchantins, macrocyclic bisbibenzyls contained in liverworts. PLoS One 6: e19825.
17. Kuzuhara T, Kise D, Yoshida H, Horita T, Murazaki Y, et al. (2009) Structural basis of the influenza A virus RNA polymerase PB2 RNA-binding domain containing the pathogenicity-determinant lysine 627 residue. J Biol Chem 284: 6855–6860.
18. Kroto HW, Heath JR, O'Brien SC, Curl RF, Smalley RE (1985) C_{60}: Buckminsterfullerene. Nature 318: 162–163.
19. Sukeguchi D, Singh SP, Reddy MR, Yoshiyama H, Afre RA, et al. (2009) New diarylmethanofullerene derivatives and their properties for organic thin-film solar cells. Beilstein J Org Chem 24: 5–7.
20. Nakamura S, Mashino T (2012) Water-soluble fullerene derivatives for drug discovery. J Nippon Med Sch 79: 248–254.
21. Bosi S, Da Ros T, Spalluto G, Prato M (2003) Fullerene derivatives: an attractive tool for biological applications. Eur J Med Chem 38: 913–923.
22. Mashino T, Shimotohno K, Ikegami N, Nishikawa D, Okuda K, et al. (2005) Human immunodeficiency virus-reverse transcriptase inhibition and hepatitis C virus RNA-dependent RNA polymerase inhibition activities of fullerene derivatives. Bioorg Med Chem Lett 15: 1107–1109.
23. Nishizawa C, Hashimoto N, Yokoo S, Funakoshi-Tago M, Kasahara T, et al. (2009) Pyrrolidinium-type fullerene derivative-induced apoptosis by the generation of reactive oxygen species in HL-60 cells. Free Radic Res 43: 1240–1247.
24. Mashino T, Nishikawa D, Takahashi K, Usui N, Yamori T, et al. (2003) Antibacterial and antiproliferative activity of cationic fullerene derivatives. Bioorg Med Chem Lett 13: 4395–4397.
25. Okuda K, Mashino T, Hirobe M (1996) Superoxide radical quenching and cytochrome c peroxidase-like activity of C_{60}-dimalonic acid, $C_{64}(COOH)_4$. Bioorg Med Chem Lett 6: 539–542.
26. Noble E, Cox A, Deval J, Kim B (2012) Endonuclease substrate selectivity characterized with full-length PA of influenza A virus polymerase. Virology 433: 27–34.
27. DuBois RM, Slavish PJ, Baughman BM, Yun MK, Bao J, et al. (2012) Structural and biochemical basis for development of influenza virus inhibitors targeting the PA endonuclease. PLoS Pathog 8: e1002830.
28. Chemical Computing Group C (2004) Molecular Operative Environment (MOE) 0707.
29. Zhao C, Lou Z, Guo Y, Ma M, Chen Y, et al. (2009) Nucleoside monophosphate complex structures of the endonuclease domain from the influenza virus polymerase PA subunit reveal the substrate binding site inside the catalytic center. J Virol 83: 9024–9030.
30. Tokuyama H, Ymago S, Nakamura E (1993) Photoinduced biochemical activity of fullerene carboxylic acid. J Am Chem Soc 115: 7918–7919.
31. Furuta Y, Takahashi K, Kuno-Maekawa M, Sangawa H, Uehara S, et al. (2005) Mechanism of action of T-705 against influenza virus. Antimicrob Agents Chemother. 49: 981–986.
32. Li L, Chang S, Xiang J, Li Q, Liang H, et al. (2012) Screen anti-influenza lead compounds that target the PA(C) subunit of H5N1 viral RNA polymerase. PLoS One. 7: e35234.
33. Cianci C, Gerritz SW, Deminie C, Krystal M (2012) Influenza nucleoprotein: promising target for antiviral chemotherapy. Antivir Chem Chemother. 10.3851/IMP2235.
34. Ishikawa Y, Fujii S (2011) Binding mode prediction and inhibitor design of anti-influenza virus diketo acids targeting metalloenzyme RNA polymerase by molecular docking. Bioinformation. 6: 221–225.
35. Nakazawa M, Kadowaki SE, Watanabe I, Kadowaki Y, Takei M, et al. (2008) PA subunit of RNA polymerase as a promising target for anti-influenza virus agents. Antiviral Res. 78: 194–201.
36. Tado M, Abe T, Hatta T, Ishikawa M, Nakada S, et al. (2001) Inhibitory effect of modified 5′-capped short RNA fragments on influenza virus RNA polymerase gene expression. Antivir Chem Chemother. 12: 353–358.
37. Nakamura Y, Oda K, Nakada S (1991) Growth complementation of influenza virus temperature-sensitive mutants in mouse cells which express the RNA polymerase and nucleoprotein genes. J Biochem 110: 395–401.
38. Mullis KB, Faloona FA (1987) Specific synthesis of DNA *in vitro* via a polymerase-catalyzed chain reaction. Methods Enzymol 155: 335–350.
39. Studier FW, Moffatt BA (1986) Use of bacteriophage T7 RNA polymerase to direct selective high-level expression of cloned genes. J Mol Biol 189: 113–130.
40. Janknecht R, de Martynoff G, Lou J, Hipskind RA, Nordheim A, et al. (1991) Rapid and efficient purification of native histidine-tagged protein expressed by recombinant vaccinia virus. Proc Natl Acad Sci U S A 88: 8972–8976.
41. Anderson D, Harris R, Polayes D, Ciccarone V, Donahue R, et al. (1996) Rapid generation of recombinant baculoviruses and expression of foreign genes using the Bac-to-Bac® baculovirus expression system. Focus 17: 53–58.
42. Morris GM, Goodsell DS, Halliday RS, Huey R Hart WE, et al. (1998) Automated docking using Lamarckian genetic algorithm and an empirical binding free energy function. J Comp Chem 19: 1639–1662.
43. Goto J, Kataoka R (2008) ASEDock-docking based on alpha spheres and excluded volumes. J Chem Inf Model 48: 583–590.
44. Takahashi E, Kataoka K, Indalao IL, Konoha K, Fujii K, et al. (2012) Oral clarithromycin enhances airway immunoglobulin A (IgA) immunity through induction of IgA class switching recombination and B-cell-activating factor of the tumor necrosis factor family molecule on mucosal dendritic cells in mice infected with influenza A virus. J Virol 86: 10924–10934.

OPEN ACCESS Freely available online

PLOS ONE

Immunomodulator Clarithromycin Enhances Mucosal and Systemic Immune Responses and Reduces Re-Infection Rate in Pediatric Patients with Influenza Treated with Antiviral Neuraminidase Inhibitors: A Retrospective Analysis

Wakako Shinahara[1], Etsuhisa Takahashi[1], Takako Sawabuchi[1], Masaru Arai[2], Nobuo Hirotsu[3], Yoshio Takasaki[4], Shizuo Shindo[5], Kyoko Shibao[6], Takashi Yokoyama[7], Kiyoshi Nishikawa[8], Masahiro Mino[9], Minako Iwaya[10], Yuji Yamashita[11], Satoshi Suzuki[12], Dai Mizuno[1], Hiroshi Kido[1]*

1 Division of Enzyme Chemistry, Institute for Enzyme Research, The University of Tokushima, Tokushima, Japan, **2** Arai Clinic, Chichibu, Japan, **3** Hirotsu Clinic, Kawasaki, Japan, **4** Takasaki Children's Clinic, Fukuoka, Japan, **5** Shindo Children's Clinic, Fukuoka, Japan, **6** Shibao Clinic, Fukuoka, Japan, **7** Yokoyama Children's Clinic, Kasuga, Japan, **8** Nishikawa Clinic, Zentsuji, Japan, **9** Mino Children's Clinic, Kannonji, Japan, **10** Iwaya Children's Clinic, Fukuoka, Japan, **11** Yamashita Children's Clinic, Maebaru, Japan, **12** Nagoya City Jouhoku Hospital, Nagoya, Japan

Abstract

Background/Aims: Treatment with antiviral neuraminidase inhibitors suppresses influenza viral replication and antigen production, resulting in marked attenuation of mucosal immunity and mild suppression of systemic immunity in mice. This study investigated the effects of immunomodulator clarithromycin (CAM) supplementation on mucosal and systemic immunity in pediatric patients with influenza treated with neuraminidase inhibitors.

Methods: A retrospective, non-randomized case series study was conducted among five treatment groups of 195 children aged 5.9±3.3 years infected with influenza A in 2008/2009 season. The five treatment groups were oseltamivir (OSV), zanamivir (ZNV), OSV+CAM, ZNV+CAM and untreated groups. Anti-viral secretory IgA (S-IgA) levels in nasal washes and IgG levels in sera were measured. The re-infection rate was analyzed among the same five treatment groups in the 2009/2010 season.

Results: Treatment of influenza with OSV and ZNV for 5 days attenuated the induction of anti-viral S-IgA in nasal washes and anti-viral IgG in serum, compared with the untreated group. The combination of CAM plus OSV or ZNV boosted and restored the production of mucosal S-IgA and systemic IgG. The re-infection rates in the subsequent season were significantly higher in the OSV and ZNV groups than the untreated, while CAM+OSV and CAM+ZNV tended to reduce such rate.

Conclusions: CAM restored the attenuated anti-viral mucosal and systemic immunity and reduced the re-infection rate in the subsequent year in pediatric patients with influenza treated with OSV and ZNV.

Citation: Shinahara W, Takahashi E, Sawabuchi T, Arai M, Hirotsu N, et al. (2013) Immunomodulator Clarithromycin Enhances Mucosal and Systemic Immune Responses and Reduces Re-Infection Rate in Pediatric Patients with Influenza Treated with Antiviral Neuraminidase Inhibitors: A Retrospective Analysis. PLoS ONE 8(7): e70060. doi:10.1371/journal.pone.0070060

Editor: Dennis W. Metzger, Albany Medical College, United States of America

Received February 17, 2013; **Accepted** June 17, 2013; **Published** July 17, 2013

Funding: This study was supported in part by a Grant in-Aid (21249061), the Special Coordination Funds for Promoting Science and Technology of Ministry of Education, Culture, Sports, Science and Technology of Japan and SENTAN Japan Science and Technology Agency. The funders had no role in study design, data collection and analysis, decision to publish, or preparation of the manuscript.

Competing Interests: The authors have declared that no competing interests exist.

* E-mail: kido@ier.tokushima-u.ac.jp.

Introduction

Influenza is a worldwide public health problem, particularly with emerging new strains to which vaccines are ineffective, limited, or unavailable. The antiviral neuraminidase inhibitors oseltamivir (OSV) and zanamivir (ZNV) are important treatment options for seasonal influenza infections [1,2], and are being stockpiled in many countries as part of their pandemic response planning. These inhibitors impair the release of new influenza virions from infected cells by blocking the actions of viral neuraminidases [2], resulting in effective suppression of viral RNA replication and viral antigen production. In contrast to the therapeutic effects of OSV, we reported recently that OSV significantly suppressed the production of mucosal antigen (Ag)-specific secretory IgA (S-IgA) antibody and Ag-specific IgA-forming cells in the mouse airway, probably due to the suppressed

viral antigen production, but it did not seriously suppress the production of systemic anti-viral IgG and IgG-forming cells in the spleen [3].

In order to prevent complications and aggravation of the flu symptoms, it is not uncommon, in Japan, to prescribe clarithromycin (CAM) developed by modification of erythromycin [4], an immunomodulator macrolide antibiotic [5–8] with antiviral activities [9,10], in combination with OSV or ZNV. In this regard, we previously reported that administration of CAM in influenza A virus (IAV)-infected mice suppressed tumor necrosis factor alpha production and augmented interleukin-12 production in the blood [11,12], resulting in alleviation of the flu symptoms, while oral treatment with OSV attenuated the induction of respiratory anti-IAV specific secretory IgA (S-IgA) immune responses [3]. Furthermore, we have verified in IAV-infected children that oral CAM augments the nasopharyngeal mucosal immune responses, while OSV suppresses the production of mucosal anti-IAV S-IgA [13]. Of interest, we have also reported that 75% of patients treated with the combination of CAM and OSV show increases in S-IgA production to levels similar to those seen in patients treated with CAM alone and untreated patients. In addition, we recently determined the molecular mechanisms responsible for the enhanced induction of mucosal IgA class switching recombination in CAM-treated mice [14]. The obtained data indicated that CAM significantly enhances the expression levels of B-cell-activating factor of the tumor necrosis factor family (BAFF) molecule on mucosal dendritic cells as well as those of activation-induced cytidine deaminase and Iμ-Cα transcripts on B cells [14]. The results indicated that CAM enhances S-IgA production through the induction of IgA class switching recombination in IAV-infected mice.

In previous clinical studies [13] on the immunomodulatory and boost effects of CAM on the nasopharyngeal mucosal immune response in pediatric patients with influenza treated with OSV, several questions remain to be answered: (i) Do antiviral neuraminidase inhibitors other than OSV, such as ZNV, an orally inhaled powder, also suppress the adaptive respiratory S-IgA response? (ii) Do the antiviral neuraminidase inhibitors also affect serum IgG responses in pediatric influenza? (iii) Do antiviral neuraminidase inhibitors, with and without CAM, affect the rate of future influenza virus re-infection? The present retrospective and non-randomized case series study was conducted to provide answers to these questions in 195 children infected with IAV. We report here that treatment with ZNV suppressed airway mucosal immunity and systemic immunity in pediatric influenza in a manner similar to OSV. The addition of CAM induced a mild boost and tended to restore the suppressed mucosal anti-viral S-IgA response in the OSV- and ZNV-treated patients, and also boosted serum IgG response, with a significant improvement in anti-IAV-specific IgG production in the ZNV-treated group. In addition, CAM tended to decrease, albeit insignificantly, the re-infection frequency in the OSV- and ZNV-treated groups.

Methods

Ethics Statement

After explanation of the purpose of this clinical study, written informed consent was obtained from each parent of pediatric patients for enrollment in the study and for the use of stored nasopharyngeal aspirates and blood for quantitative analyses of anti-IAV antibodies. Permission to perform clinical studies and ethical approval of the study protocol were granted by the Ethics Committee of Tokushima University Hospital (Permit Number, #463). The study was conducted under the supervision of the pediatricians involved (MA, NH, YT, SS, KS, TY, KN, MM, MI, YY and SS), and parents were advised of risks, benefits and the right to withdraw their children from further involvement in the study at any point without repercussions. All data, particularly patient identification data, were physically and electronically secured throughout the study.

Study population

The study subjects were 195 children (age, 5.9±3.3 years, mean±SD, range, 0–14 years), who were infected with IAV between October 2008 through March 2009 in 11 Pediatric Clinics and Children's Hospitals in the mid-west region of Japan. A descriptive survey study on re-infection was conducted for the same children from October through March of 2009/2010. The inclusion criteria were the followings: patients who presented to the Pediatric Clinics and Children's Hospitals and diagnosed with the rapid diagnosis Espline Influenza A&B-N kit (Fujirebio Inc., Tokyo, Japan) and whose treatment was initiated within 48 hours of the onset of fever. Patients with congenital defects and those with co-morbid chronic diseases were excluded. Since the number of Japanese infected with influenza B in the 2008/2009 season was not large [15], and the antigen of influenza B/Victoria lineage prevailing in the season was not commercially available for the analysis of antibody titers, statistical analysis was conducted only on data of patients who presented with IAV.

Treatment regimens

Patients diagnosed with IAV infection were divided into five groups according to the prescription of each pediatrician involved: the no-treatment group (n = 68), the OSV group (70 patients treated orally twice daily with OSV at 2 mg/kg body weight for 5 days), OSV+CAM group (20 patients treated orally twice daily with OSV at 2 mg/kg body weight for 5 days plus oral CAM at 5.0–7.5 mg/kg body weight for 5 days), the ZNV group (27 patients older than 4 years treated twice daily with orally inhaled ZNV powder at 10 mg for 5 days) and ZNV+CAM group (10 patients treated twice daily with orally inhaled ZNV powder at 10 mg for 5 days plus oral CAM at 5.0–7.5 mg/kg body weight for 5 days). There were no outbreaks of *Mycoplasma* or *Chlamydia* at the time of the study. All patients were followed for 5 days.

Collection of biological samples

All children suspected clinically to have influenza underwent both nasopharyngeal aspiration and serum collection. Nasopharyngeal aspiration was conducted on each nostril for 1 minute, through a silicon tube, and the aspirate collected in a centrifuge tube connected to an evacuator, as described previously [16,17]. The isolated specimens were immediately cooled on ice, homogenized by sonification for 20 seconds on ice, in a model 250, 20% duty, 2-cycle Sonifier® (Branson Ultrasonics Co., Danbury, CT), and the insoluble materials were removed by centrifugation at 2000× *g* for 5 minutes at 4°C. The supernatants of nasopharyngeal specimens and serum were stored at −30°C until use.

Enzyme-linked immunosorbent assay (ELISA)

The concentrations of total IgA, IgG and anti-IAV-specific S-IgA in nasopharyngeal specimens and anti-IAV-specific IgG in sera were measured by ELISA, as described previously [13,17]. For measurement of anti-IAV-specific antibody, the prevalent IAV strains were selected as coating ELISA antigens: In the 2008/2009 flu season before May 2009, IAV/Brisbane/59/2007(H1N1)-like and IAV/Uruguay/716/2007(H3N2)-like subtypes were prevalent in Japan [15]. Since the affinity purified human anti-IAV-specific

S-IgA and IgG standards for each IAV subtypes are not commercially available, the concentrations of anti-IAV-specific antibody in the nasopharyngeal specimens and sera were determined from the standard regression curves with human IgA and IgG of known concentrations in a human IgA and IgG quantitation kits (Bethyl Laboratories Inc., Montgomery, TX). The relative values of anti-IAV-specific S-IgA and IgG were expressed as units (U); one U of each anti-IAV-specific S-IgA and IgG was determined from the regression curves as the point corresponding to 1 μg of human IgA and 1 mg of human IgG detected in the assay system, respectively, as described previously [13,17]. Since the concentration of nasal wash samples varies widely between individuals depending on the aspiration efficiency and patient age, the concentration of anti-IAV-specific S-IgA (U/mL) was normalized by the amount of protein (mg/mL). Since there was no significant variability in serum protein concentrations, the row values of anti-IAV-specific IgG concentrations (U/mL) were used. The protein concentrations in the nasopharyngeal specimens were measured using a bicinchoninic acid protein assay reagent kit (Pierce, Rockford, IL).

Statistical analysis

Results are presented as the median (interquartile range), or numbers (%) of observations. The S-IgA levels in nasopharyngeal specimens of the different patient groups were compared by the Mann-Whitney U-test and Wilcoxon signed-rank test. Between group comparisons of disease symptoms were made using Fisher's exact test with the Bonferroni correction. A P value <0.05 was considered statistically significant.

Results

Patient characteristics

Table 1 lists the characteristics of patients of the five groups. The most common features of influenza were fever (defined as body temperature ≥38°C), sore throat, cough, nasal discharge, headache and body aches. About half (48.6–64.7%) of the patients in each group had received vaccination before the onset of the influenza season and no significant differences in the values were observed among the five groups. The prevalence of disease signs and symptoms at admission to hospital was similar among the five groups. The time between onset of illness and initial examination ranged from 1.0 to 1.9 days with a mean value of 1.7±0.6 days.

Effects of OSV and ZNV on nasopharyngeal antiviral-S-IgA production and serum antiviral-IgG in patients treated with or without CAM

Table 2 summarizes the levels of anti-IAV(H1N1)- and (H3N2)-specific S-IgA (U/mg protein) and total S-IgA (μg/mg protein) before and 5 days after treatment with OSV and ZNV, with or without CAM. In the control (no treatment) group, significant increases in the concentrations of anti-IAV-specific S-IgA against subtypes H1N1 ($P<0.05$) and H3N2 ($P<0.01$) were observed at 5 days after infection. The percentages of patients with greater than or equal (≥1-fold) to baseline titer before treatment and greater than or equal to a four-fold increase (≥4-fold) from baseline titer in the no-treatment group against subtype H1N1 were 61.5 and 26.2, respectively, and against subtype H3N2 were 69.2 and 15.4, respectively. Treatment with OSV and ZNV significantly suppressed the percentage of patients with ≥1-fold of baseline titer against both H1N1 and H3N2 subtypes, compared with the values in the no-treatment group. However, co-administration of CAM and OSV boosted S-IgA induction and increased the percentage of patients with ≥1-fold of baseline titer from 42.9 to 65.0 against H1N1 and from 42.9 to 70.0 against H3N2 (P value versus OSV group for H1N1: $P<0.06$ to <0.09, H3N2: <0.05). Co-administration of CAM and ZNV resulted in mild restoration of the suppressed percentage of patients with ≥1-fold of baseline titer from 37.0 to 50.0 against H1N1 and from 48.1 to 60.0 against H3N2, although the differences between the two were not statistically significant. There were no significant differences in the percentages of patients with ≥4-fold of baseline S-IgA titer among the five treatment groups.

Table 3 lists the levels of serum anti-IAV(H1N1)- and (H3N2)-specific IgG (U/mL) and total IgG (mg/mL) before and 5 days after treatment of IAV infection with OSV and ZNV, with or without CAM. Significant increases were noted in serum levels of anti-IAV-specific IgG in all groups at 5 days after treatment, except those against H1N1 in the OSV and ZNV groups. In particular, ZNV treatment significantly reduced the percentage of patients with ≥1-fold of baseline titer against H1N1 compared with the no-treatment group, from 73.5 to 40.9 ($P<0.01$), in a manner similar to that noted in mucosal S-IgA responses. In addition, the combination of CAM plus ZNV significantly increased the percentage of patients with ≥1-fold of baseline titer against H1N1 ($P<0.01$), though the increase against H3N2 was

Table 1. Patient characteristics.

	All patients	No Treatment	OSV	OSV+CAM	ZNV	ZNV+CAM
	(n = 195)	(n = 68)	(n = 70)	(n = 20)	(n = 27)	(n = 10)
Age, years, (range)*	5.9±3.3 (0–14)	7.3±3.9 (0–14)	4.2±2.7 (0–10)	5.1±2.1 (1–9)	7.0±1.6 (5–9)	6.9±2.0 (4–9)
Time between onset illness and initial examination (days)*	1.7±0.6	1.6±0.7	1.7±0.6	1.9±0.6	1.6±0.6	1.0±0.7
Previous vaccination (%)	112(57.4)	44(64.7)	34(48.6)	12(60.0)	17(63.0)	5(50.0)
Fever (%)	180(95.2)	63(92.6)	68(100)	16(88.9)	25(96.2)	8(88.9)
Sore throat (%)	68(35.4)	24(35.3)	20(29.9)	4(20.0)	15(55.6)	5(50.0)
Cough (%)	173(88.7)	64(94.1)	61(87.1)	16(80.0)	23(85.2)	9(90.0)
Nasal discharge (%)	177(90.8)	67(98.5)	64(91.4)	17(85.0)	20(74.1)	9(90.0)
Headache (%)	70(36.6)	26(38.2)	20(30.3)	4(20.0)	14(51.9)	6(60.0)
Body aches (%)	54(28.7)	16(23.5)	24(37.5)	3(15.8)	8(29.6)	3(30.0)

*Data are mean±SD.

doi:10.1371/journal.pone.0070060.t001

Table 2. Changes in anti-IAV-specific S-IgA production in untreated patients and patients treated with OSV and ZNV for 5 days, with or without CAM.

Treatment	n	S-IgA concentration						Percentage of patients with ≥1-fold and ≥4-fold increases in anti-IAV-specific S-IgA concentration during treatment			
		Anti-IAV-specific S-IgA (U/mg protein)				Total S-IgA (μg/mg protein)					
		H1N1		H3N2				H1N1		H3N2	
		Before	After	Before	After	Before	After	≥1-fold (After/before)	≥4-fold (After/before)	≥1-fold (After/before)	≥4-fold (After/before)
No treatment	65	2.3 (0.5–5.7)	3.1 (1.2–7.8)*	2.2 (0.6–3.8)	3.1 (1.0–6.7)[¶]	120.6 (90.3–177)	143.5 (118–204)*	61.5	26.2	69.2	15.4
OSV	70	1.3 (0.6–5.9)	1.2 (0.4–5.0)	1.0 (0.4–2.8)	1.1 (0.5–3.1)	122.8 (79.1–147)	128.0 (82.8–163)	42.9[§]	18.6	42.9[‡]	14.3
OSV+CAM	20	0.9 (0.3–1.4)	1.9 (0.3–12.3)*	0.7 (0.2–1.7)	1.5 (0.3–7.6) [¶]	121.6 (74.1–153)	134.1 (98.9–214)*	65.0[#]	30.0	70.0[†]	20.0
ZNV	27	3.8 (1.7–12.3)	4.5 (0.5–15.8)	2.0 (1.4–3.8)	2.6 (0.5–7.8)	109.7 (86.8–181)	149.8 (101–216)	37.0[§]	18.5	48.1[§]	11.1
ZNV+CAM	10	2.0 (1.6–7.1)	6.3 (2.2–19.5)	1.7 (1.2–2.4)	4.3 (1.8–11.6)	143.3 (104–202)	173.2 (151–207)	50.0	30.0	60.0	30.0

Data are median (interquartile range). Before and after denote before and after treatment, respectively.
*$P<0.05$,
[¶]$P<0.01$, versus before treatment for the same parameter (Wilcoxon signed-ranks test).
[§]$P<0.05$, versus the respective no treatment (Fisher's exact test). [‡]$P<0.01$, versus the respective no treatment (Fisher's exact test).
[#]$P<0.06$ to <0.09, versus the OSV group (Fisher's exact test). [†]$P<0.05$, versus the OSV group (Fisher's exact test).
doi:10.1371/journal.pone.0070060.t002

Table 3. Changes in anti-IAV-specific IgG production in untreated patients and patients treated with OSV and ZNV for 5 days, with or without CAM.

Treatment	n	IgG concentration						Percentage of patients with ≥1-fold and ≥4-fold increases in anti-IAV-specific IgG concentration during treatment			
		Anti-IAV-specific IgG (U/mL)				Total IgG (mg/mL)					
		H1N1		H3N2				H1N1		H3N2	
		Before	After	Before	After	Before	After	≥1-fold (After/before)	≥4-fold (After/before)	≥1-fold (After/before)	≥4-fold (After/before)
No treatment	49	0.5 (0.2–0.9)	0.8 (0.4–1.5)[¶]	0.4 (0.2–0.7)	0.8 (0.3–1.4)[¶]	19.3 (10.9–48.3)	17.7 (10.2–28.1)*	73.5	30.6	73.5	34.7
OSV	52	0.2 (0.03–0.7)	0.5 (0.06–1.0)	0.2 (0.04–0.5)	0.4 (0.06–1.1)[¶]	13.2 (9.1–17.6)	11.8 (8.6–17.4)	63.5	21.2	75.0	32.7
OSV+CAM	14	0.5 (0.3–0.6)	0.9 (0.5–1.4)[¶]	0.5 (0.2–0.5)	0.6 (0.4–1.2)*	14.1 (10.1–21.1)	12.0 (9.6–16.7)	78.6	21.4	85.7	14.3
ZNV	22	0.6 (0.3–1.1)	0.6 (0.4–1.1)	0.3 (0.2–0.5)	0.5 (0.4–0.9)[¶]	11.9 (8.3–31.4)	15.3 (9.4–28.4)	40.9[‡]	13.6	68.2	18.2
ZNV+CAM	8	0.3 (0.2–0.6)	0.9 (0.2–1.8)*	0.4 (0.2–0.7)	1.4 (0.4–2.6)*	15.4 (10.2–22.0)	12.0 (8.9–14.9)	100.0[†]	25.0	100.0[#†]	50.0

Data are median (interquartile range). Before and after denote before and after treatment, respectively.
*$P<0.05$,
[¶]$P<0.01$, versus before treatment for the same parameter (Wilcoxon signed-ranks test).
[‡]$P<0.01$, versus the respective no treatment (Fisher's exact test).
[#]$P<0.06$ to <0.09, versus the ZNV group (Fisher's exact test).
[†]$P<0.01$, versus the ZNV group (Fisher's exact test).
doi:10.1371/journal.pone.0070060.t003

marginal, ($P<0.06$ to <0.09), compared with ZNV alone. There were no significant differences in the percentages of patients with ≥4-fold of baseline IgG titer among the five treatment groups.

Table 4 compares the prevalence of disease manifestations at day 5 after treatment. Significant improvements were noted in the prevalence of cough in the OSV+CAM group, compared with the OSV group ($P<0.05$), and nasal discharge in the ZNV+CAM group, compared with the ZNV group ($P<0.05$). However, there were no significant differences in the effects of various treatments on the other listed symptoms among the five treatment groups.

Frequency of re-infection in subsequent year

Based on the low level of acquired mucosal anti-IAV-specific S-IgA after infection, patients were at risk of re-infection in the subsequent year, particularly those treated with OSV or ZNV. Figure 1 lists the percentages of re-infected individuals according to the treatment received in the preceding year. The IAV pH1N12009 was the predominant circulating virus in Japan with a peak during October-December of 2009. Even under the spread of a new virus subtype in the 2009/2010, only 8.6% of the children of the no-treatment group were re-infected. However, the proportions of children treated the previous year with OSV and ZNV who developed re-infection in 2009–2010 were significantly higher at 37.3% and 45.0%, respectively ($P<0.01$), than those of the no-treatment group. The combination treatment of CAM plus OSV and CAM plus ZNV tended to reduce the re-infection rate to 17.6% and 22.2%, respectively, albeit insignificantly.

Discussion

The main findings of the present study were the following: (i) Treatment with antiviral neuraminidase inhibitors, OSV and ZNV, tended to suppress the production of respiratory anti-IAV-specific S-IgA as well as systemic anti-IAV-specific IgG in pediatric patients with influenza. (ii) The combination treatment of CAM plus OSV or ZNV mildly or significantly enhanced the production of anti-IAV S-IgA in the nasopharyngeal specimens and/or anti-IAV IgG in sera and tended to restore the suppressed local mucosal and systemic immunity observed with antiviral inhibitor agents. (iii) The rates of IAV re-infection in the subsequent year were significantly higher for the OSV and ZNV groups than the control group, whereas the combination of CAM plus OSV or ZNV tended to reduce such rate.

There is general agreement that the first line of host defense against infection is mucosal immunity, particularly nasopharyngeal immunity, which constitutes a major component of the immunological humoral and cell-mediated responses in the upper and lower respiratory tracts [18,19]. However, the currently available intramuscularly and subcutaneously-injected influenza vaccines predominantly induce systemic IgG but not S-IgA and weak cellular immunity in the airway mucosa [18–21]. In fact, the levels of anti-IAV S-IgA relative to the total sIgA were low in nasal washes of all influenza patients on admission, whereas serum levels of anti-IAV IgG levels varied widely, probably reflecting the history of infection and vaccination in these individuals [13,17]. Treatment of pediatric influenza with OSV or ZNV for 5 days significantly suppressed acquired anti-IAV S-IgA levels in nasal washes (Table 2) and these changes may also explain the higher frequency of re-infection in the OSV and ZNV groups in the subsequent year (Figure 1). The results may be supported by previous findings that mucosal S-IgA is primarily involved in cross-protection of the mucosal surface against variant IAV infection, and the mechanism of broad-spectrum cross-protection could be explained by the wide-range cross-reactivity of S-IgA [22–25].

The suppressive effects of OSV and ZNV on mucosal anti-IAV S-IgA levels, probably due to diminution of viral antigen production by anti-viral neuraminidase inhibitors, seem to be ameliorated by co-administration of CAM. CAM boosted mucosal and/or systemic immunity and tended to increase the levels of anti-IAV S-IgA in nasal washes and IgG in serum in the OSV- and ZNV-treated patients (Tables 2 and 3). This effect of CAM resulted in an increase in the percentage of patients with ≥1-fold of baseline titer before treatment, particularly S-IgA in the OSV-treated patients and IgG in the ZNV-treated patients. Although patients of the ZNV group were slightly older (about 2 years) than those of the OSV group, because of age limitation of oral inhalation of ZNV powder, the observed effects of ZNV on mucosal and systemic immunity were similar to those of OSV with or without CAM. The effects of OSV and ZNV with or without CAM could be clearer in naïve children with low or undetectable pre-existing immunological memory. The present results emphasize the need to study the effects of CAM in adult patients with pre-existing immunological memory and elderly patients with low immunological responses.

Nasopharyngeal-associated lymphoreticular tissue is known as the production site of nasal S-IgA, where IgA-committed B cells undergo class switching. Subsequently, IgA-committed B cells migrate to mucosal effector tissues including the nasal passages [26]. We reported recently that CAM enhances IgA class switching recombination through upregulation of BAFF in mucosal dendritic cells and activation-induced cytidine deaminase in B cells [14]. The present clinical results add support to these early studies.

Table 4. Rates of improvement of clinical symptoms after 5 days of no treatment and treatment with OSV, OSV+CAM, ZNV and ZNV+CAM.

Improvement (%)	Fever	Sore throat	Cough	Nasal discharge	Headache	Body aches
No treatment (n = 68)	94.1 (64/68)	92.0 (23/25)	35.4 (23/65)	41.5 (27/65)	96.0 (24/25)	100 (16/16)
OSV (n = 70)	94.3 (66/70)	68.2 (15/22)	31.3 (20/64)	39.4 (26/66)	100 (21/21)	100 (26/26)
OSV+CAM (n = 20)	95.0 (19/20)	80.0 (4/5)	58.8* (10/17)	61.1 (11/18)	100 (4/4)	100 (4/4)
ZNV (n = 27)	96.3 (26/27)	93.3 (14/15)	50.0 (12/24)	37.5 (9/24)	86.7 (13/15)	87.5 (7/8)
ZNV+CAM (n = 10)	100 (10/10)	100 (5/5)	60.0 (6/10)	77.8† (7/9)	100 (6/6)	100 (3/3)

Data are percentage of patients who reported disappearance of symptoms per patients with symptoms at the start of treatment.
*$P<0.05$, versus OSV (Fisher's exact test).
†$P<0.05$, versus ZNV (Fisher's exact test).
doi:10.1371/journal.pone.0070060.t004

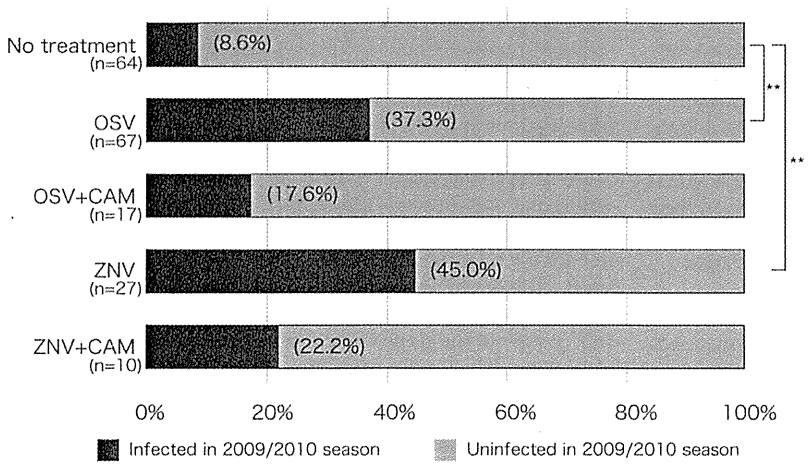

Figure 1. Re-infection rate in 2009/2010 season. The re-infection rate in 2009/2010 season in children who were infected with IAV during the 2008/2009 season and either untreated or treated with OSV, OSV+CAM, ZNV and ZNV+CAM. Data show the percentage of infected children in each group. *$P<0.05$, * *$P<0.01$, versus no treatment (Fisher's exact test with Bonferroni correction).
doi:10.1371/journal.pone.0070060.g001

In conclusion, the present study showed that CAM boosts and tends to restore the suppressed mucosal and/or systemic immunity in pediatric patients with influenza treated with OSV and ZNV.

Author Contributions

Conceived and designed the experiments: HK WS. Performed the experiments: MA NH YT SS KS TY KN MM MI YY SS. Analyzed the data: WS ET TS DM. Contributed reagents/materials/analysis tools: WS ET TS DM. Wrote the paper: HK WS.

References

1. Moscona A. (2005) Neuraminidase inhibitors for influenza. N Engl J Med 353:1363–1373.
2. Ison MG. (2011) Antivirals and resistance: influenza virus. Curr Opin Virol 1: 563–573.
3. Takahashi E, Kataoka K, Fujii K, Chida J, Mizuno D, et al. (2010) Attenuation of inducible respiratory immune responses by oseltamivir treatment in mice infected with influenza A virus. Microbes Infect 12:778–783.
4. Hashisaki GT. (1995) Update on macrolide antibiotics. Am J Otolaryngol 16:153–157.
5. Kudoh S, Uetake T, Hagiwara K, Hirayama M, Hus LH, et al. (1987) Clinical effects of low-dose long-term erythromycin chemotherapy on diffuse panbronchiolitis. Nihon Kyobu Shikkan Gakkai Zasshi 25:632–642.
6. Labro MT. (2001) Anti-inflammatory activity of macrolides: a new therapeutic potential? Antimicrob Agents Chemother 45:44–47.
7. Suzuki T, Yamada M, Sekizawa K, Hosoda M, Yamada N, et al. (2002) Erythromycin inhibits rhinovirus infection in cultured human tracheal epithelial cells. Am J Respir Crit Care Med 165:1113–1118.
8. Tahan F, Ozcan A, Koc N. (2007) Clarithromycin in the treatment of RSV bronchitis: a double-blind, randomized placebo-controlled trial. Eur Respir J 29:91–97.
9. Sato K, Suga M, Akaike T, Fujii S, Muranaka H, et al. (1998) Therapeutic effect of erythromycin of influenza virus-induced lung injury in mice. Am J Respir Crit Care Med 157:853–857.
10. Maeda S, Yamada Y, Nakamura H, Maeda T. (1999) Efficacy of antibiotics against influenza-like illness in an influenza epidemic. Pediatr Int 41:274–276.
11. Kido H, Okumura Y, Yamada H, Le TQ, Yano M. (2007) Protease essential for human influenza virus entry into cells and their inhibitors as potential therapeutic agents. Curr Pharm Des 13:405–414.
12. Tsurita M, Kurokawa M, Imakita M, Fukuda Y, Watanabe Y, et al. (2001) Early augmentation of interleukin (IL)-12 level in the airway of mice administrated orally with clarithromycin or intranasally with IL-12 results in alleviation of influenza infection. J Pharmacol Exp Ther 298:362–368.
13. Sawabuchi T, Suzuki S, Iwase K, Ito C, Mizuno D, et al. (2009) Boost of mucosal secretory immunoglobulin A response by clarithromycin in paediatric influenza. Respirology 14:1173–1179.
14. Takahashi E, Kataoka K, Indalao IL, Konoha K, Fujii K, et al. (2012) Oral clarithromycin enhances airway immunoglobulin A (IgA) immunity through induction of IgA class switching recombination and B-cell-activating factor of the tumor necrosis factor family molecule on mucosal dendritic cells in mice infected with influenza A virus. J Virol 86:10924–10934.
15. Infectious Disease Surveillance Center, National Institute of Infectious Diseases of Japan. (2009) 2008/09 influenza season, Japan. Infect Agents Surveill Rep 30:285–286. Available: http://idsc.nih.go.jp/iasr/30/357/tpc357.html. Accessed May 31, 2013.
16. Fujimoto C, Kido H, Sawabuchi T, Mizuno D, Hayama M, et al. (2009) Aspiration of nasal IgA secretion in normal subjects by nasal spray and aspiration. Auris Nasus Larynx 36:300–304.
17. Fujimoto C, Takeda N, Matsunaga A, Sawada A, Tanaka T, et al. (2012) Induction and maintenance of anti-influenza antigen-specific nasal secretory IgA levels and serum IgG levels after influenza infection in adults. Influenza Other Respi Viruses 6:396–403.
18. Holmgren J, Czerkinsky C. (2005) Mucosal immunity and vaccines. Nat Med 11:S45–53.
19. Doherty PC, Topham DJ, Tripp RA, Cardin RD, Brooks JW, et al. (1997) Effector CD4$^+$ and CD8$^+$ T-cell mechanisms in the control of respiratory virus infection. Immunol Rev 159:105–117.
20. Clements ML, Betts RF, Tierney EL, Murphy BR. (1986) Serum and nasal wash antibodies associated with resistance to experimental challenge with influenza A wild type virus. J Clin Microbiol 24:157–160.
21. Mizuno D, Ide-Kurihara M, Ichinomiya T, Kubo I, Kido H. (2006) Modified pulmonary surfactant is a potent adjuvant that stimulates the mucosal IgA production in response to the influenza virus antigen. J Immunol 176:1122–1130.
22. Nishino M, Mizuno D, Kimoto T, Shinahara W, Fukuta A, et al. (2009) Influenza vaccine with Surfacten, a modified pulmonary surfactant, induces systemic and mucosal immune responses without side effects in minipigs. Vaccine 27:5620–5627.
23. Murphy BR, Clements ML. (1989) The systemic and mucosal immune response of humans to influenza A virus. Curr Top Microbiol Immunol 146:107–116.
24. Liew FY, Russell SM, Appleyard G, Brand CM, Beale J. (1984) Cross-protection in mice infected with influenza A virus by the respiratory route is correlated with local IgA antibody rather than serum antibody or cytotoxic T cell reactivity. Eur J Immunol 14:350–356.
25. Renegar KB, Small PA Jr, Boykins LG, Wright PF. (2004) Role of IgA versus IgG in the control of influenza viral infection in the murine respiratory tract. J Immunol 173:1978–1986.
26. Kunkel EJ, Butcher EC. (2003) Plasma-cell homing. Nat Rev Immunol 3:822–829.

OPEN ACCESS Freely available online

PLOS ONE

Diisopropylamine Dichloroacetate, a Novel Pyruvate Dehydrogenase Kinase 4 Inhibitor, as a Potential Therapeutic Agent for Metabolic Disorders and Multiorgan Failure in Severe Influenza

Kazuhiko Yamane[1], Irene L. Indalao[1], Junji Chida[1], Yoshikazu Yamamoto[2], Masaaki Hanawa[2], Hiroshi Kido[1]*

1 Division of Enzyme Chemistry, Institute for Enzyme Research, The University of Tokushima, Tokushima, Japan, **2** R&D Department, Daiichi Sankyo Healthcare Co., Ltd., Tokyo, Japan

Abstract

Severe influenza is characterized by cytokine storm and multiorgan failure with metabolic energy disorders and vascular hyperpermeability. In the regulation of energy homeostasis, the pyruvate dehydrogenase (PDH) complex plays an important role by catalyzing oxidative decarboxylation of pyruvate, linking glycolysis to the tricarboxylic acid cycle and fatty acid synthesis, and thus its activity is linked to energy homeostasis. The present study tested the effects of diisopropylamine dichloroacetate (DADA), a new PDH kinase 4 (PDK4) inhibitor, in mice with severe influenza. Infection of mice with influenza A PR/8/34(H1N1) virus resulted in marked down-regulation of PDH activity and ATP level, with selective up-regulation of PDK4 in the skeletal muscles, heart, liver and lungs. Oral administration of DADA at 12-h intervals for 14 days starting immediately after infection significantly restored PDH activity and ATP level in various organs, and ameliorated disorders of glucose and lipid metabolism in the blood, together with marked improvement of survival and suppression of cytokine storm, trypsin up-regulation and viral replication. These results indicate that through PDK4 inhibition, DADA effectively suppresses the host metabolic disorder-cytokine cycle, which is closely linked to the influenza virus-cytokine-trypsin cycle, resulting in prevention of multiorgan failure in severe influenza.

Citation: Yamane K, Indalao IL, Chida J, Yamamoto Y, Hanawa M, et al. (2014) Diisopropylamine Dichloroacetate, a Novel Pyruvate Dehydrogenase Kinase 4 Inhibitor, as a Potential Therapeutic Agent for Metabolic Disorders and Multiorgan Failure in Severe Influenza. PLoS ONE 9(5): e98032. doi:10.1371/journal.pone.0098032

Editor: Amy Lynn Adamson, University of North Carolina at Greensboro, United States of America

Received January 23, 2014; **Accepted** April 28, 2014; **Published** May 27, 2014

Funding: This research was funded in part by Grants-in-Aid (#24249059) from the Ministry of Education, Culture, Sports, Science, and Technology of Japan; by Health and Labor Sciences Research Grants (Grant #12103307) from the Ministry of Health, Labor and Welfare of Japan. The funding agencies have no role in the study design, data collection and analysis, decision to publish, or preparation of the manuscript.

Competing Interests: YY and MH are employed by Daiichi Sankyo Healthcare Co., Ltd. Their jobs are product planners. In this study, they provided diisopropylamine dichloroacetate, together with chemical and medical information on the product. HK, KY, JC, YY and MH are inventors of an applied patent on diisopropylamine dichloroacetate (patent application #WO 2012/101846 A1), entitled "Therapeutic or prophylactic agent for influenza". The patent is co-owned by the University of Tokushima and Daiichi Sankyo Healthcare Co., Ltd. The publication of the data reported here is at the discretion of the University of Tokushima. The authors confirm that Daiichi Sankyo Healthcare Co., Ltd did not control the data presented in this manuscript or interpretation of the data within the paper. This does not alter the authors' adherence to all the PLOS ONE policies on sharing data and materials. The other authors declare no competing interests.

* E-mail: kido@ier.tokushima-u.ac.jp

Introduction

Influenza A virus (IAV) is the most common infectious pathogen in humans and causes significant morbidity and mortality, particularly in infants and elderly population [1,2]. Multiorgan failure (MOF) with severe edema is reported in the progressive stage of seasonal influenza virus pneumonia and influenza-associated encephalopathy, particularly in patients with underlying risk factors [3–5] and is common in the highly pathogenic avian IAV infection [6]. The antiviral neuraminidase inhibitors are used for treatment in the initial stage of IAV infection and a 5-day course of these compounds is recommended for individuals with flu symptoms of not more than 2 days. A proportion of individuals with progressive symptoms after the initial stage of infection develop MOF with metabolic disorders and vascular hyperpermeability. To date, the pathogenesis and treatment target molecules of MOF by IAV remain poorly understood.

We reported previously that the influenza virus–cytokine–trypsin cycle is one of the main underlying mechanisms of vascular hyperpermeability and MOF in severe influenza [7]. Severe influenza causes marked increases in the levels of proinflammatory cytokines, such as tumor necrosis factor (TNF)-α, interleukin (IL)-6, and IL-1β, coined the cytokine storm. These cytokines alter the cellular redox state through their receptors and reduce the expression of four complex I subunits, oxygen consumption [8,9] and ATP synthesis in mitochondria, as well as increase mitochondrial O_2- production and intracellular calcium concentration $[Ca^{2+}]_i$ [10]. ATP depletion dissociates zonula occludens-1, intracellular tight junction component, from the actin cytoskeleton and increases junctional permeability [11]. These cytokines also upregulate trypsin, which mediates the post-translational proteo-

lytic cleavage of viral envelope hemagglutinin and is crucial for viral entry and replication cycle [12], in various organs and endothelial cells. Trypsin also increases $[Ca^{2+}]_i$ and enhances loss of zonula occludens-1 in cells via the protease-activated receptor (PAR)-2 [7,13,14]. In addition, we reported recently that metabolic disorders and energy crisis in brain endothelial cells by IAV infection are the main mechanisms of influenza-associated encephalopathy, which is characterized in infancy and early childhood in East Asian countries by persistently high fever and severe brain edema [5,15,16]. Patients with influenza-associated encephalopathy exhibit thermal instability of compound variants for [1055T>G/F352C] and [1102G>A/V368I] of carnitine palmitoyltransferase II (CPT II), resulting in secondary CPT II deficiency and mitochondrial energy crisis through disorders of long-chain fatty acid metabolism during hyperpyrexia. These findings indicate that MOF is the final outcome of metabolic and mitochondrial fuel disorders in severe influenza, although the precise signaling pathways involved in these disorders are still unknown.

The mitochondrial pyruvate dehydrogenase (PDH) complex (PDC) catalyzes the oxidative decarboxylation of pyruvate, linking glycolysis to the energetic and anabolic functions of the tricarboxylic acid cycle and fatty acid synthesis via acetyl-CoA. Therefore, PDC is a key enzyme for regulation of whole body glucose, lipid, lactate and ATP homeostasis. PDC is a structurally complex enzyme of three components [PDH (E1), dihydrolipoamide acetyltransferase (E2), and dihydrolipoamide dehydrogenase (E3)] with two specific regulatory enzymes, pyruvate dehydrogenase kinases (PDKs) 1–4 for phosphorylation (inactivation) of the α-subunit of PDH and pyruvate dehydrogenase phosphate phosphatases (PDPs) 1 and 2, for dephosphorylation (activation, reactivation) of the α-subunit of PDH [17,18]. Expression of PDKs is linked to homeostasis of glucose, lipid, lactate, ATP, cytokines, and hormone levels in various diseases and suppressively regulates PDH activity [17–20].

In the present study, we describe selective and marked up-regulation of PDK4, an isoform of PDK, together with down-regulation of PDH activity and ATP levels in the skeletal muscles, heart, liver and lungs, but not the brain, in mice with the progressive stage of severe influenza and cytokine storm conditions. The results also showed that diisopropylamine dichloroacetate (DADA), which is the active component of pangamic acid [21] and commercially available as a Liverall (Daiichi Sankyo Co., Tokyo, Japan) for over 50 years for the treatment of chronic liver diseases, is a safe inhibitor of PDK4. DADA selectively and effectively inhibited PDK4, resulting in significant restoration of PDH activity as well as various metabolic disorders, such as ATP levels in various organs, and improved glucose, lactate and β-hydroxybutyric acid levels in the blood. Amelioration of PDH suppression in the infected mice by DADA was associated with significant vital improvements, such as restoration of energy metabolism, suppression of cytokine storm and viral proliferation, with marked improvement of survival.

Methods

Reagents

DADA was obtained from Daiichi Sankyo Healthcare Co. (Tokyo). Sodium DCA was purchased from Wako Pure Chemical Industries (Osaka, Japan).

Animals and virus

All animals were treated according to the Guide for the Care and Use of Laboratory Animals (NIH Publication No. 85–23, 1996), and the study was approved by the Animals Care Committee of the University of Tokushima. Specified pathogen-free 4-week-old weanling C57BL/6CrSlc (B6) female mice were obtained from Japan SLC and maintained at 12-h light/dark cycle in a temperature-controlled room with free access to food and water. IAV/PR/8/34(H1N1) was kindly provided by The Research Foundation for Microbial Diseases of Osaka University (Kagawa, Japan). Under ketamine and xylazine anesthesia, 60, 120 and 200 plaque-forming units (pfu) of IAV/PR/8/34(H1N1) in 15 μL of saline or saline alone as non-infected control was instilled intranasally in mice. Mice were treated orally with DADA, a PDK inhibitor, starting immediately after infection at 50 mg/kg at 12-h intervals for 14 days in 100 μL sterilized 0.5% methylcellulose 400 (MC) solution mixed with calcium gluconate, a food additive, in commercially available medicine format at 4.68 mg/mL. The dose of DADA was adjusted to yield daily molar doses similar to the range of DCA used clinically (clinical doses, 25–100 mg/kg/day [22,23]). Positive control mice were treated with intraperitoneal injection of 100 μL of DCA at 28 mg/kg, an equivalent molar dose to DADA, at 12-h intervals daily. Mice were monitored daily for body weight and food and water intake and assessed visually for signs of clinical diseases including inactivity, ruffled fur, labored respiration and huddling behavior. Mice that lost ≥30% of their original body weight and/or displayed evidence of pneumonia were euthanized by overdose of intraperitoneal injection of ketamine and xylazine.

Blood glucose, lactate, free fatty acids and β-hydroxybutyric acid assays

Whole blood levels of glucose, lactate, and β-hydroxybutyric acid were measured according to the protocols recommended by Medisafe-Mini GR-102 (Terumo, Japan), Lactate-Pro LT-1710 (Arkray, Japan) and Precision Xceed (Abbot, Japan) hand-held meter, respectively. Serum levels of free fatty acids were measured according to the protocols provided with the Free Fatty Acid Quantification Kit (Abcam, Japan).

Blood and tissues ATP assays

Tissue ATP levels were measured by the firefly bioluminescence assay kit with an improved phenol-based ATP extraction reagent [24] (AMERIC-ATP (T) kit; Wako Pure Chemical Industries) according to the protocol supplied by the manufacturer. Freshly prepared brain, heart, lungs, liver and skeletal muscle (gastrocnemius muscle) tissues were homogenized immediately with 3.0 mL of ice-cold phenol-based ATP extraction reagent by Ultra-Turrax (Ika Japan, Nara, Japan). The tissue ATP levels were normalized against wet-tissue weight. Blood ATP levels were also measured by AMERIC-ATP kit for blood and cells using the procedure described previously [25].

IC_{50} analysis

The half maximal inhibitory concentrations (IC_{50}) of DADA and DCA against human PDK2 and PDK4 recombinant proteins expressed baculovirus system were measured by the method of off-chip mobility shift assay using a panel of human recombinant active kinases [26] from Carna Biosciences, Inc. (Kobe, Japan).

PDH activity

PDH activity was measured in the brain, heart, lungs, skeletal muscles, and liver by the PDH Enzyme Activity Microplate Assay Kit (MSP18) (MitoSciences, Eugene, OR). The PDH was immunocaptured within the microplate and activity was determined by following the reduction of NAD^+ to NADH, coupled to

the reduction in a reporter dye color. Tissues homogenates in PBS(-) were prepared by Dounce Tissue Grinder to avoid mitochondrial damage. Tissue samples were then solubilized and diluted with detergent in the assay kit at the optimal protein concentrations for each organ to immunocapture PDH on the microplate; brain (1 mg/well), heart (200 μg/well), lungs (1 mg/well), liver (800 μg/well) and muscles (1 mg/well). After adding the reaction mixture, absorbance was monitored at 450 nm for 15 min. The activity was expressed as the initial rate of reaction.

Western immunoblotting

Anti-mouse PDK4 antibody (provided generously by Dr. M. Horiuchi, Kagoshima University, Japan), was used for detection of PDK4 in the heart, lungs, skeletal muscles and liver tissues [27]. Freshly isolated tissues were homogenized with 7 volumes of RIPA lysis buffer containing 50 mM Tris-HCl, pH 8.0, and 150 mM NaCl, 10% glycerol, 1% NP 40, 0.5% deoxycholate, 0.4 mM EDTA, and 0.5 mM sodium orthovanadate (Thermo Scientific, Yokohama, Japan) and centrifuged at 12,000×*g* for 20 min. The extracts (with protein concentration of 16.7 μg) were used for immunoblotting, as described previously [13]. Immunoreactive bands were visualized by enhanced chemiluminescence detection system (GE Healthcare, Tokyo) and the detected bands were quantified by ImageJ software.

Real-time PCR

Total RNA was extracted from mice tissues with RNeasy Mini kit (Qiagen, Hilden, Germany) and reverse transcribed using oligo primers and universal primers in SuperScript III RT kit (Gibco BRL, Grand Island, NY) for cDNA synthesis. RT-PCR and quantification of gene expression by real-time PCR were performed using a Fast Start Universal SYBR Green Master (Roche Diagnostics, Mannheim, Germany) on an ABI Prism 7300 system. The primer pairs used to amplify influenza A virus NS1, PDK1–4, PDP 1–2, trypsin and mouse glyceraldehyde-3-phosphate dehydrogenase (GAPDH) are listed in Table 1. PCR was initiated at 95°C for 10 min to activate HotStartTaq DNA polymerase, followed by 40 cycles of 30-s denaturation at 95°C, 30-s annealing at 52°C and 50-s extension at 72°C.

Enzyme-linked immunosorbent assay (ELISA)

The lung samples were crushed with 3 mL PBS and IL-6, IL-2, TNF-α, IL-1β, and IFN-γ levels in the homogenates were measured using Quantikine ELISA kit (R&D systems, Minneapolis, MN). IFN-α and IFN-β levels were measured using VeriKine ELISA kits (R&D systems) according to the respective protocols provided by the manufacturer.

Histological evaluation

After euthanasia, the lungs were isolated then fixed with 4% paraformaldehyde, dehydrated, infiltrated, and cut into 5-μm paraffin-embedded tissue sections for histological evaluation, as described previously [13]. Tissue sections were stained with hematoxylin–eosin.

Statistical analysis

Results are presented as mean ± SD. Differences between groups were analyzed by one-way analysis of variance (ANOVA) with Tukey post hoc test. Survival rate was analyzed by the Kaplan-Meier and log-rank tests. Changes in body weight among groups were analyzed by two-way ANOVA. All statistical tests were performed using the Microsoft Excel software (Microsoft Corp, Redmond, WA) add-in Ekuseru-Toukei 2010 version 1.10 (Social Survey Research Information Co.). All *P* values are two-sided, and those less than 0.05 were considered statistically significant.

Results

Low PDH activity and ATP levels in various organs of mice infected with sub-lethal doses of IAV infection

Intranasal administration of 60 pfu of IAV PR/8/34(H1N1) in 15 μL of saline in 4-week-old B6 mice was semi-lethal by day 14 post-infection; the animals began to die after day 7 post-infection. Furthermore, 120 pfu was sub-lethal with 3–5% survival rate. Animals administered 200 pfu began to die after day 7 post-infection and all were dead (100% mortality rate) by day 10 (lethal dose). At day 4 post-infection and thereafter, the majority of animals infected with these doses of IAV developed clinical signs of infection (e.g., inactivity, loss of body weight, ruffled fur, labored respiration and huddling behavior). MOF starts at day 4 post-IAV-infection, and is characterized by marked increase in the levels of proinflammatory cytokines and a rapid increase in viral proliferation via the influenza virus–cytokine–trypsin cycle [7,12]. After peak viral proliferation in the lung at days 4 to 5 post-infection, various metabolic disorders associated with cellular dysfunction become obvious in various organs, together with the initiation of host protective immunity [12].

Mice infected with 120 pfu of IAV had significantly low PDH activity in the lungs at day 3 post-infection (to about 50–60% of the non-infected control) and also in the skeletal muscles, liver and

Table 1. Sequences of primers used in real-time PCR.

Gene	Forward primer (5′-3′)	Reverse primer (5′-3′)
PDP1	CGGGCACTGCTACCTATAATT	ACAATTTGGACGCCTCCTTACT
PDP2	GGCTGAGCATTGAAGAAGCATT	GCCTGGATTTCTAGCGAGATGT
PDK1	CCGGGCCAGGTGGACTTC	GCAATCTTGTCGCAGAAACATAAA
PDK2	GCTTCCCCTGACCTGGAGAT	AGGCTGGACTCGGCTTT
PDK3	CGGTCCCCAAGCAGATCGA	GTTAGCCAGTCGCACAGGAG
PDK4	CACATGCTCTTCGAACTCTTCAAG	TGATTGTAAGGTCTTCTTTCCCAAG
Trypsin	AGTGGGTGGTGTCTGCAGCTCA	GATTCCTGCCAGGGTGACTC
NS-1	TACCTGCGTCGCGTTACCTAA	TGCTTCTCCAAGCGAATCTCT
GAPDH	CATCACCATCTTCCAGGA	GAGGGGGCCATCCACAGTCTTC

doi:10.1371/journal.pone.0098032.t001

heart at day 7 post-infection (Figure 1A). On the other hand, PDH activity in the brain remained unchanged at days 3 and 7 post-infection. ATP levels in the heart, lungs, skeletal muscles and liver, but not in the brain, showed similar reduction patterns (both time course and tendency, Figure 1B). These findings indicate that sub-lethal doses of IAV induce significant disorder of glucose oxidation, reduction of energy metabolism, and poor ATP generation in the skeletal muscles, liver, lungs and heart, through reduction of PDH activity in the mitochondria.

IAV infection induces marked and selective up-regulation of PDK4 in the skeletal muscles, heart, lungs and liver

Oxidative decarboxylation of pyruvate involves three structurally complex enzymes, including PDH (E1), E2, and E3, that catalyze the conversion of pyruvate to acetyl-CoA [17,18]. The complex also contains two specific phosphorylation-dephosphorylation enzymes; PDK and PDP. Table 2 shows changes in relative mRNA expression levels of these regulatory compounds in the liver, heart, lungs, skeletal muscles and brain at days 0, 3 and 7 post-infection. Although a sub-lethal dose of IAV infection was associated with variable changes in the expression of these phosphorylation-dephosphorylation enzymes, marked and predominant up-regulation of PDK4 was evident in the skeletal muscles, liver, lungs and heart. However, up-regulation of PDK4 in the brain was very mild even at day 7 post-infection. Western immunoblotting analysis (Figure 2) confirmed predominant up-regulation of PDK4 protein with a peak at day 3 post-infection in the lungs, and peaks at day 7 post-infection in the skeletal muscles, heart and liver. Changes in protein levels in these organs were almost identical to those in mRNA levels.

DADA as a novel PDK4 inhibitor

A sub-lethal dose of IAV up-regulates PDKs, particularly PDK4, resulting in the suppression of PDH activity in the mitochondria (Table 2, Figures 1 and 2). Among the known synthetic inhibitors of PDK [28], such as dichloroacetate (DCA), AZD7545 and radicicol, the pyruvate analog DCA is the most common classic inhibitor for PDK isoforms [29]. In the present study, we analyzed the inhibitory activity of DADA, a DCA derivative and commercially-available safe compound, against PDK4 and PDK2, which are the main PDK isoforms in the skeletal muscles, heart, lungs and liver [20], and used DCA as a positive control in these experiments (Table 3). Kinetic studies showed that the IC_{50} values, i.e., DADA concentrations at which the reaction rates are suppressed by 50%, were 50.9 μM against PDK4 and 636.0 μM against PDK2. These values were almost identical to those of DCA against PDK4 and PDK2, respectively. These results indicate that DADA is a novel PDK4 inhibitor with about 12.5-fold higher affinity than that against PDK2.

DADA significantly increases PDH activity and ATP levels in the skeletal muscles, heart, lungs and liver

To analyze the effects of DADA as a PDK4 inhibitor on PDH activity and ATP levels in different tissues, mice infected with a sub-lethal dose of IAV PR/8/34(H1N1) were treated orally with DADA immediately after the infection, at 50 mg/kg twice daily. As described above, the infection resulted in marked suppression of PDH activities and ATP levels at day 7 post-infection, the time point before animal death, in the skeletal muscles, liver, lungs and heart to about 25–52% and 48–63% of the non-infected control, respectively (Figure 3). DADA significantly prevented the effects of

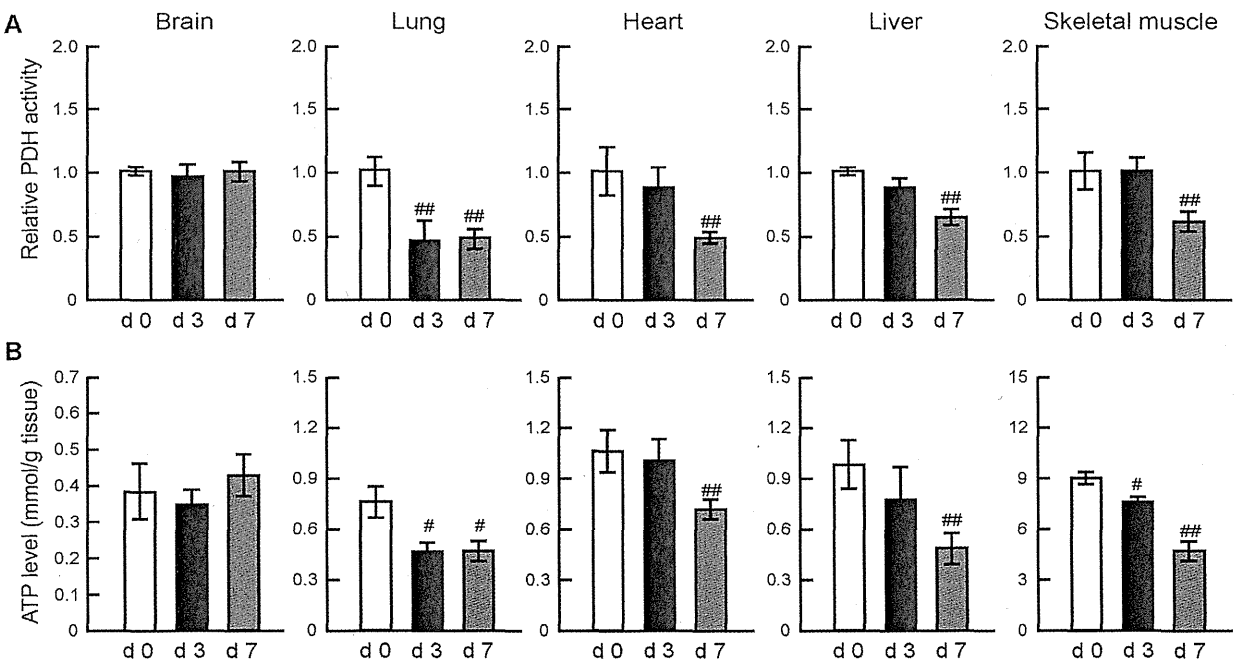

Figure 1. Time course of changes in PDH activity and ATP levels in the skeletal muscles, heart, lungs, liver and brain of IAV-infected mice. Mice were infected with IAV/PR/8/34(H1N1) at 120 pfu intranasally and the levels of PDH activity (A) and ATP (B) in the skeletal muscles, heart, lungs, liver and brain were analyzed at days 0 (d0), 3 (d3) and 7 (d7) post-infection. PDH activity levels after IAV infection relative to the values at day 0. Data are mean ± SD of 5 mice per group. $^{\#}P<0.05$, $^{\#\#}P<0.01$ vs. day 0, by one-way analysis of variance (ANOVA) with Tukey post hoc test.
doi:10.1371/journal.pone.0098032.g001